NIST Technical Note 1802

Characterizing the Response of Direct-Reading Particulate Detectors for the Fire Overhaul Environment

Rodney A. Bryant
Paul S. Greenberg

National Institute of Standards and Technology
U.S. Department of Commerce

NIST Technical Note 1802

Characterizing the Response of Direct-Reading Particulate Detectors for the Fire Overhaul Environment

Rodney A. Bryant
Fire Research Division
Engineering Laboratory

Paul S. Greenberg
Glenn Research Center
National Aeronautics and Space Administration

June 2013

U.S. Department of Commerce
Cameron F. Kerry, Acting Secretary

National Institute of Standards and Technology
Patrick D. Gallagher, Under Secretary of Commerce for Standards and Technology and Director

National Institute of Standards and Technology Technical Note 1802
Natl. Inst. Stand. Technol. Tech. Note 1802, 46 pages (June 2013)
CODEN: NTNOEF

EXECUTIVE SUMMARY

The overhaul of a fire scene is a stage of firefighting where respiratory protection is often disregarded due to the perception of low risk for respiratory injury. The operation resembles a structural demolition, with the added presence of smoldering debris. Limited information exists on what respiratory threats remain. Hand-held direct-reading particulate detectors have long been used to monitor respiratory threats for industrial hygiene applications. Therefore, it may be possible to adapt this technology to meet the needs of the firefighter.

Even though direct-reading particulate detectors have been used for quite some time, there is not a consensus standard for evaluating worker exposure as a function of the device output. There is a diversity of particles present in the fire overhaul environment and their characteristics significantly differ depending on the scenario. Optical direct-reading instruments are sensitive to the physical characteristics of the particles, which presents many challenges for accurately detecting particulates during fire overhaul.

The goal of the present work was to conduct a preliminary characterization of hand-held direct-reading particulate detectors when exposed to the types of particulates anticipated in the fire overhaul environment, and to transfer the knowledge gained into recommendations that will provide the foundation for future research, standards development, and testing protocols specific to the needs of the firefighter community.

Four optical dust monitors, representative of those currently available on the market, were simultaneously exposed to smoke surrogates and smoke from burning materials to characterize their response. The response from the dust monitors was linear over the range of particle mass concentrations for current exposure threshold limits. However, the sensitivity varied with respect to the aerosol for some of the detectors. When exposed to smoke from burning materials, the response of the dust monitors did not adequately reflect the hazard present. Some burning materials produced very high particle number concentration, which could be a significant respiratory hazard. The dust monitors' output was in terms of mass concentration and did not always indicate the presence of the hazard.

Key recommendations for performance evaluation metrics and testing protocols include:

1. Evaluating dust monitors to confirm a linear response of over the range of the current respiratory threshold limits, 0 mg/m^3 to 10 mg/m^3.
2. Using a condensation particle counter to generate a reference measurement of particle occurrence that is independent of particle characteristics such as size, shape, and refractive index.
3. Using the cone calorimeter and standard test method ASTM E 1354-11a to generate real smoke particles.

Key recommendations for improvements in direct-reading detector technology include:

1) A dual device, one that can measure mass concentration and number concentration simultaneously, would be ideal. When small particles dominate, mass concentration is low. Measurements of number concentration can still reflect the presence of a hazard.

2) Adding an internal or external dilution system to optical particle counters to allow more of the devices to operate in high particle concentration environments like fire overhaul.

Key recommendations for future research include:

1. Investigating the use of aerosolized mineral oil to calibrate dust monitors for use in the fire overhaul environment.
2. Identifying a comprehensive list of flammable materials found in buildings beyond the list considered here to create aerosols that characterize the full range of refractive index that may be encountered during overhaul.

Keywords: fire overhaul, respiratory protection, particulate detection, aerosol detection, fire safety, first responder, firefighter

ACKNOWLEDGMENTS

The Science and Technology Directorate of the U.S. Department of Homeland Security (DHS) sponsored the production of this material under Interagency Agreement HSHQDC-09-X-00476 with the National Institute of Standards and Technology (NIST). The authors wish to thank the following NIST staff and student interns for their valuable contributions: Mr. Marco Fernandez (NIST Technician) for fabricating the experimental equipment as well as conducting experiments; Mr. Matthew Sakofs (Summer Undergraduate Research Fellowship Student, Univ. of Maryland) for data analysis; Mr. Olatunde Sanni (Student Intern, Univ. of Maryland) for conducting experiments and data analysis; and Mr. John Shields (NIST Technician) for conducting the cone calorimeter experiments.

Table of Contents

INTRODUCTION

The overhaul of a fire scene is a stage of firefighting where respiratory protection is often disregarded due to a perception of low risk and the desire to remove the heavy and cumbersome self-contained breathing apparatus. The overhaul operation occurs after the immediately visible fire has been extinguished and involves searching for and exposing hidden pockets of fire to ensure that the fire is completely extinguished. The operation resembles a structural demolition, with the added presence of smoldering debris. Limited information exists on what respiratory threats are present during this stage of firefighting. The need for alternatives for respiratory protection that are fitted to the task and the environment has been voiced by the firefighter community [1] and studies have recommended that some level of respiratory protection should be implemented. [2,3] Choosing the appropriate respiratory protection for individual events can only be accomplished with real-time information about the exposure hazards. Hand-held direct-reading particulate detectors have been used in other environmental monitoring applications, and it may be possible to adapt the technology to meet the needs of the firefighter.

Direct-reading particulate detectors are considered a compliment to traditional filter-based gravimetric methods for exposure monitoring of work environments. Even though these instruments have been used for quite some time, there is not a consensus standard for evaluating worker exposure using direct-reading particulate detectors. Only in recent years has a best practice guide been developed for optical particle counters for workplace exposure. [4,5] Optical direct-reading instruments are sensitive to the physical characteristics of the particles. Depending on the measurement techniques, some characteristics can be exploited while others introduce measurement error. It is recommended to calibrate the instruments for the specific aerosol and that the physical characteristics of the aerosol remain stable during the exposure assessment. Unfortunately, there is a diversity of particulates present in the fire overhaul environment and their characteristics differ depending of the scenario. Therefore this presents many challenges for accurately detecting particulates during fire overhaul.

To explore the potential for using hand-held direct-reading particulate detectors to aid firefighters during overhaul, the Department of Homeland Security sponsored a workshop on Real-Time Particulate Monitoring. The workshop was held at the National Institute of Standards and Technology (NIST) in May 2007. [6] Members of the fire service, particulate detector manufacturers, public health professionals, aerosol researchers, fire science researchers, and standards organizations convened to discuss the need for better technology to assess the level of respiratory protection required for work by firefighters in the overhaul environment. The consensus among workshop participants was that additional research is needed to better understand the health effects of particulates on firefighters, to better characterize the particulates present during overhaul, and to better characterize the response of particulate detectors to the overhaul environment.

The goal of the present work is to conduct a preliminary characterization of hand-held direct-reading particulate detectors when exposed to the types of particulates anticipated in the fire overhaul environment. The characterization was conducted using the current state-of-the-art hand-held devices. The knowledge gained by characterizing the response of the detectors for this unique environment provides the foundation for future research, standards development, and testing protocols specific to the needs of the firefighter community.

BACKGROUND

Aerosols

Concentration and Exposure

Respiratory exposure to an aerosol (*a suspension of solid or liquid particles in a gas*) is a combination of two factors: i) the concentration of the aerosol itself, and ii) the length of the time of exposure. This combination is expressed in equation 1:

$$\text{Total Dose} = (\text{Aerosol concentration}) \times (\text{Time of Exposure}) \quad (1)$$

The concentration of an aerosol can be expressed in several ways. For example, the concentration can be specified as the number of particles that are found in some specified volume (e.g. per cubic foot, per cubic meter, etc.). Although the total number of particles in the volume is one way of expressing concentration, other properties of the particles can also be used. For example, each particle in the volume has a certain amount of mass. From the perspective of respiratory health, the total mass of all the particles together in a specified volume is traditionally the most common way of characterizing the concentration of an aerosol. This concentration shall be referred to as $C_M(V)$, where the subscript M denotes the total amount of mass contributed by all the particles contained in the volume (V). Specifically:

$$C_M(V) = \text{Aerosol mass concentration} = \text{Total mass} / \text{unit volume} \quad (2)$$

The standard for concentration used here was adopted by the American Conference of Governmental Industrial Hygienists, Inc. (ACGIH). [7,8] Specifically, this standard specifies a maximum permissible exposure, expressed as the total amount of mass of particles contained in one cubic meter. This concentration defines the allowable, time-average mass concentration that can be encountered in a continuous eight hour period. In this standard, the total mass is expressed in units of grams. This exposure limit is referred to as the TLV, or Threshold Limit Value. ACGIH guidelines for TLV are 3 milligrams per cubic meter for respirable particulates and 10 milligrams per cubic meter for inhalable particulates. Particulates deposited in the gas-exchange or alveolar region of the respiratory system are defined as respirable, while those that enter the nose or mouth and can deposit anywhere in the respiratory tract are defined as inhalable.

Distributions

Sources of respirable particles associated with fire overhaul and emergency response situations do not produce particles of a single size (monodisperse). Rather, they result in a broad, or polydisperse Particle Size Distribution (PSD). Referring to Figure 1, there are two important characteristics that describe a PSD. These two readily apparent features describe where the peak in the PSD occurs, and the width of the distribution. Since conventional limits in respiratory exposure concern the mass of the associated aerosols, Figure 1 shows the mass-weighted PSD. Instead of graphically indicating the relative *number* of each particle size present in the distribution, this representation shows the amount of *mass* contributed by each different particle size. Figure 1 shows the Mass Median Diameter (MMD). The median connotes that the PSD contains equal amounts of mass above this value as it does below. For this particular PSD, the

MMD does not coincide exactly with the peak of the distribution, although its location can be associated with the location of the peak. This will be discussed in more detail shortly.

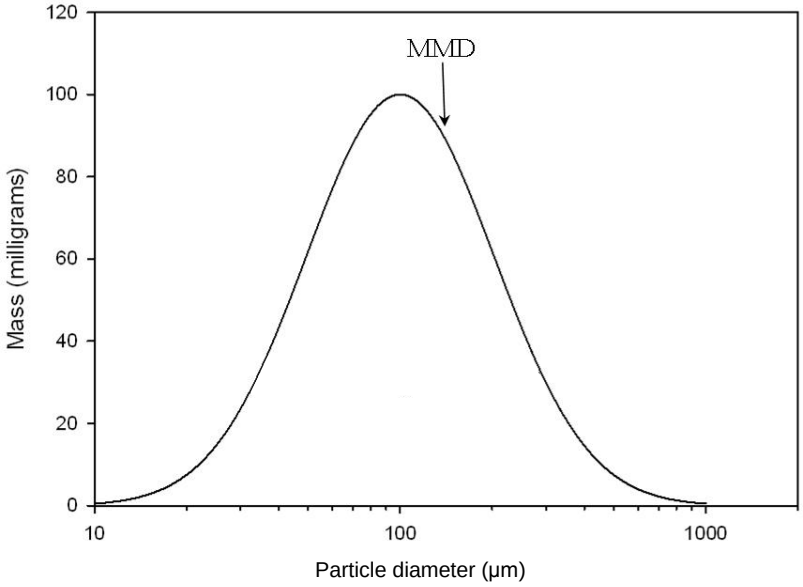

Figure 1 Sample mass-weighted particle size distribution (PSD).

The width of the PSD is customarily described by the symbol σ_g, and is defined mathematically as the geometric standard deviation (GSD). Setting aside the precise mathematical expression, the GSD describes the region of the PSD that contains roughly 70 % of the total number of particles. In this plot, σ_g also describes the region of the PSD that contains roughly 70 % of the total mass of this aerosol.

Characterizing the performance of particle measuring instruments requires a set of test aerosols with precisely specified and reproducible PSDs. Data collected on a very large number of aerosols produced from a broad variety of sources reveals that many individual aerosols can be accurately described by a lognormal PSD. The exact mathematical expression for a lognormal PSD is as follows:

$$dN = \frac{N}{\sqrt{2\pi}\ln\sigma_g}\exp\left[\frac{-(\ln d_p - \ln CMD)^2}{2(\ln\sigma_g)^2}\right]d(\ln d_p) \qquad (3)$$

where:

d_p = particle diameter
σ_g = geometric standard deviation
dN = number of particles of diameter d_p
N = total number of particles
CMD = Count Median Diameter

The Count Median Diameter (CMD) that appears in equation 3 is analogous to the Mass Median Diameter. In this case, the PSD contains the same number of particles above this value as it does below. For lognormal PSDs, the CMD and MMD are simply related:

$$MMD = CMD \exp(3\ln^2\sigma_g) \quad (4)$$

The PSD shown in Figure 1 is a lognormal distribution. Note that when the x-axis (or particle size axis) is plotted on a logarithmic scale, the PSD appears symmetric. Note also that the MMD does not coincide with the peak of the PSD, but is slightly offset. The peak in the number distribution is called the Mode Diameter, and is equal to: $CMD \exp(-\ln^2\sigma_g)$.

For most aerosols of general interest, the CMD is in the range of approximately 0.2 μm to 4.0 μm, and σ_g is in the range of 1.2 to 3.0. Specific values of interest for the testing purposes discussed here will be addressed when describing the characteristics of individual instruments and how they respond.

The Respirable Fraction

To this point, the PSD has been taken to describe the ambient aerosol, or the aerosol as it occurs naturally in the environment. In actuality, the TLV standard does not describe the ambient aerosol, but rather the portion of an ambient aerosol that is deposited in the gas-exchange region of the lung (also referred to as the alveolar region). Much attention has been devoted to the amount and size of particles that penetrate to various levels within the respiratory tract as a whole. The Respirable Fraction describes the fraction of particles of a given size [in an ambient aerosol] that penetrate into the respirable region of the lung. This relationship is shown graphically in Figure 2. [8,9]

In general, laboratory reference instruments are designed to the best degree possible to make unbiased measurements. Specifically, the intent is to accurately sample and measure ambient aerosols. The situation is somewhat different, however, for instruments intended for industrial hygiene or environmental health applications. In this case, the desire is to characterize human exposure, or more specifically, the Respirable Fraction. For instruments intended for this type of application, the input sampling probes are intentionally designed to replicate the behavior illustrated graphically in Figure 2. In this fashion, the instrument provides a measure of the Respirable Fraction ostensively deposited in the alveolar region of the lung. As will be discussed, this penetration function is an important factor when modeling the expected response of various aerosol measuring instruments.

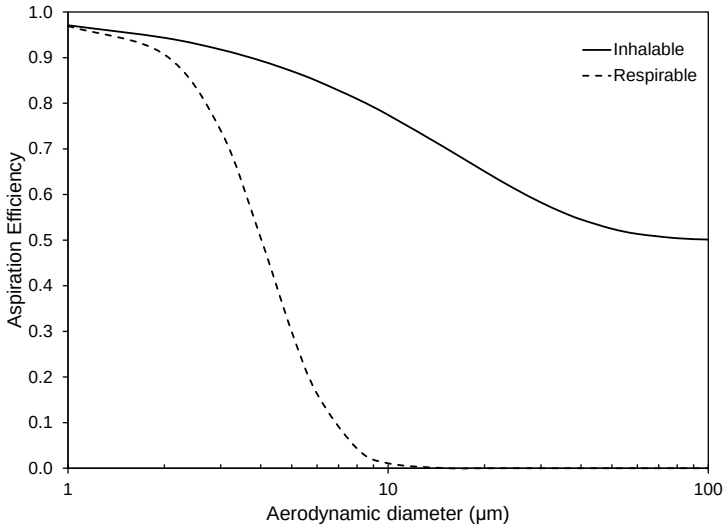

Figure 2 Standard convention for the Respirable Fraction.

This consideration is illustrated in Figure 3. Here is shown the PSD of an aerosol with a MMD of 4.2 µm and a σ_g of 2.0. The solid line illustrates the mass distribution versus particle size for the naturally occurring, or ambient aerosol. In contrast, the dotted line is the respirable fraction of this same aerosol. In this example, the respirable fraction contains roughly 54 % as much mass as the ambient aerosol, a significant difference.

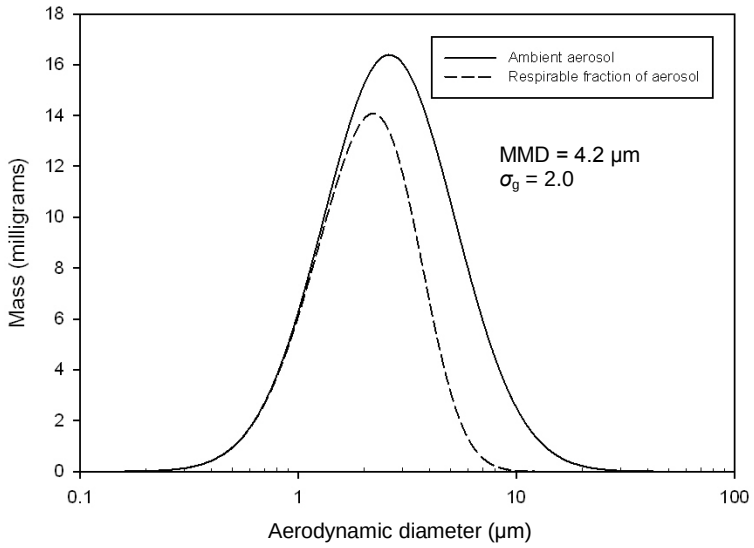

Figure 3 Comparison of mass-weighted PSDs for ambient aerosol and Respirable Fraction.

Physical Properties

Particle size will affect the accuracy of an instrument, but other properties may also affect the accuracy of a given instrument in measuring a given aerosol. As will be discussed, there are several types of commercially available instruments for this purpose. Since these devices are

based on a variety of different measurement techniques, their accuracies are affected in different ways depending on particle properties.

In addition to size, the other main properties that may influence the measurement are:

- Shape
- Density
- Optical refractive index

Variations in these properties will affect the readings from different types of devices. It should be noted that the environment of interest here, fire overhaul, will generally contain a mixture of particles. Therefore, it is important to consider how an individual instrument will respond to a combination of particle properties that are present simultaneously. Again it is emphasized that current standards for respiratory exposure are not based on the number of particles in the aerosol or their specific size, but rather on the total respirable mass.

Aerosol Measuring Instruments

Traditionally, particulate exposure limits have been quoted as mass concentration (mg/m^3). The mass concentration of aerosolized matter is most reliably determined by passing a known volume of gas through a filter and determining the increase in mass of the filter due to the amount of particulates deposited on the filter. Determining particulate mass concentration by accurately weighing the filter before and after sampling is simple, accurate and widely used. However, analysis requires a substantial amount of time since it requires the use of a sensitive microbalance, typically at a location different from the sample location. Direct-reading instruments can provide almost real-time results, within seconds to minutes depending on the sampling time and the nature of the instrument. The class of direct-reading instruments considered here are optical instruments that measure particle mass, size, or occurrence indirectly from light scattering. In terms of mass response, these instruments tend to be less accurate than gravimetric filter measurements, but their rapid delivery of results allows one to measure environments that are changing, and to correlate the change with the measurements.

The detection and characterization of aerosolized particles can be accomplished by exploiting their optical properties. Because the particles' optical properties differ from that of the surrounding air, incident light is both scattered and absorbed by the particles. In principle, both the scattering and absorption effects can be utilized for particle measurements. However, because many particles of interest absorb very weakly, optical scattering provides a more practical basis for measurement instruments. Two properties of the light scattered by particles are generally used to measure their size and concentration: i) the total amount of light that is scattered, and ii) the geometry, or pattern exhibited by the scattered light. Both properties carry information regarding the size and the concentration of the aerosol. The recent advent of extremely compact, low cost, and reliable solid-state laser sources (laser diodes) and optical detectors (PIN (semiconductor) diodes) has led to the availability of a wide array of portable field devices to measure the size and concentration of aerosol particles.

The basic construction of an optical particle detector is shown in Figure 4. An aerosol sample is first drawn into the instrument, at a specific volume flow rate, by way of an internal pump. The flow is continuous and typically set at several liters per minute. The sampled aerosol stream is then illuminated by a light source located within the instrument. Suitable optics are used to focus the light from the source onto the sample. One or more detectors are then used to collect the light scattered by the particles. The scattered light provides information about both the size and number of particles. Depending on the sophistication of the instrument, a number of detectors may be employed, to increase its accuracy or range. The output of the detector(s) is then processed by an internal computer, which computes the concentration of the sample, and in some cases, by particle size. This information is then logged into the instrument's memory. In many devices, the logged information includes the volume of the sample that is collected and the time of collection.

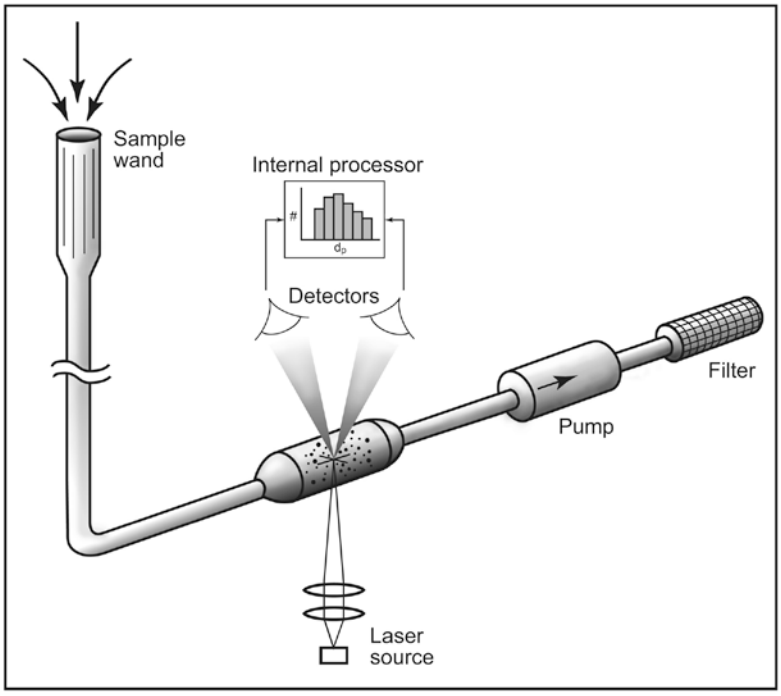

Figure 4. Schematic of the basic construction of a hand-held particle detector.

Optical Dust Monitors

One class of instrument is the aerosol or dust monitor, typically reporting concentration as mass/volume. It is designed to measure the total mass of the aerosolized particles, since mass is often used as a measure for evaluating exposure. In a dust monitor, the light scattered from a sample of particles is collected. The total mass of the sample is proportional to how many particles the sample contains, so a dust monitor measures mass by adding up the scattered light contributed by all of the particles together. Thinking more about how the mass of a group of spheres is determined, it is possible to understand that the total mass in the sample not only depends on how many spheres (particles) there are, but it depends on how big they are as well (the mass of each sphere being proportional to the cube of its diameter). In reality, the amount of light scattered by a particle is only approximately proportional to the cube of its diameter, so this

aspect affects the ability of a dust monitor to measure mass accurately. Commercially available instruments are capable of measuring mass concentration over the range of 0.001 mg/m^3 to 400 mg/m^3 over a particle size range of 0.1 μm to 10 μm. Most instruments are calibrated by comparing the instrument response to a standard dust, such as the ISO Test Dust, with standard gravimetric measurements. [10] Because the light scatter depends on the physical and optical properties of the aerosol, the calibration does not guarantee that the instrument will respond accurately to other aerosols. Therefore, when the properties of the aerosol are unknown, which is likely the case for field measurements, filter sample gravimetric measurements are recommended by manufacturers for direct comparison to calibrate the instrument to the specific aerosols in the environment.

Optical Particle Counters

Optical particle counters (OPCs) are one class of instruments that use light to measure aerosol particles. Specifically, OPCs measure the amount of light that is scattered by each individual particle. It is important to note that this approach essentially measures the particle's size. Because the interest is the respirable mass of an aerosol, using an OPC requires assumptions to be made about the density of the particles in question. Since the mass of a particle is proportional to its density, any error made in the incoming assumption of particle density will result in a proportional error in the measurement of the total mass of the aerosol. In the fire overhaul environment, it is seldom known what specific particle materials are present, and many materials are likely to be present simultaneously. This presents a fundamental challenge in using an OPC to measure total respirable mass.

The basic concept of an OPC is straightforward. The amount of light that a particle scatters is related to its size. An OPC measures this scattered light, and compares the result to a pre-established calibration table. This table is typically compiled by the manufacturer using reference particles of known size and optical refractive index. As will be seen, it is important to emphasize that an OPC measures individual particles one at a time. It should also be noted that OPCs are calibrated using spherical particles. The amount of light scattered by non-spherically shaped particles is a complex phenomena, beyond the level of detail presented here.

An example of an OPC calibration table is shown in Figure 5. In this case, the values of scattered power were not obtained experimentally, but computed directly using a physical model for optical scattering. The geometry of the collection optics considered in this calculation is typical for some types of OPCs.

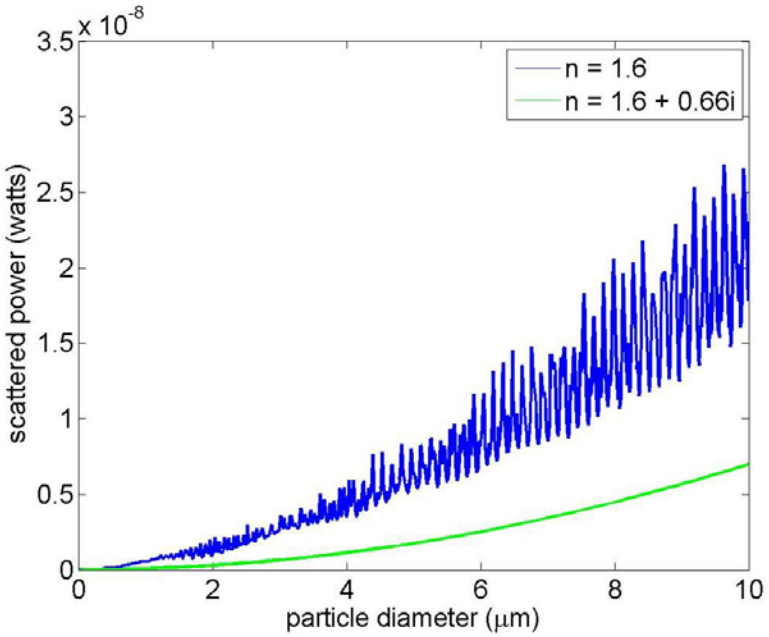

Figure 5 Scattered power versus particle size for a typical OPC.

A few features are readily apparent from Figure 5. For both curves, the amount of scattered power clearly varies as a function of the particle size. The two curves depict two different particle materials. Each material possesses an inherent optical refractive index, denoted as n. The refractive index of a given particle fundamentally affects the manner in which light is scattered. The upper, or blue, curve corresponds to a value of refractive index typical for pyrolysis products, essentially oily hydrocarbon droplets. The lower, or green, curve corresponds to carbonaceous soot characteristic of flaming combustion. For this case, the refractive index n = 1.6 + 0.66i. The second term (0.66i) is a mathematical way of expressing the fact that these particles scatter light, but absorb a portion of the light as well.

The oscillatory behavior of the upper blue curve in Figure 5 results from the complexities of light scattering from particles. Small changes in particle size greatly affect the angular distribution of the scattered light (in this case, the portion of the scattered light that reaches the optical detector). These rapid fluctuations introduce uncertainty into the OPC measurement; since by virtue of the calibration table, a given value of scattered power does not uniquely coincide with a single value of particle diameter. However, most OPCs display their measurements in terms of bins, e.g. the number of particles occurring in the bin from (1 to 5) μm, the bin from (5 to 10) μm, etc. Since many particles are grouped together in a bin, the effect of these oscillations tends to average out for the bin as a whole.

As seen in the lower curve, these oscillations are damped for particles that also absorb as well as scatter light. The more important consequence here is the observed difference in the amount of scattered light for these two types of particles. Depending on the refractive index of the particles that are used to calibrate the OPC, the instrument will tend to over or under predict the actual particle size when the refractive index differs as shown in Figure 5. In this particular case, the magnitude of this error at 10 μm is a factor of 2 to 3. Since this represents an error in the measurement of diameter, the associated error in the measurement of mass is 2^3 to 3^3 (since the

mass of a particle is proportional to the cube of its diameter). In some cases, an OPC may be calibrated using several different types of particles, and the associated calibration tables are user selectable. However, such a feature may not be useful if the composition of the particles in a given environment is not known, or if several types of particles are present simultaneously.

Within the class of OPCs are instruments called Condensation Particle Counters (CPC). This class of instruments is capable of extending the lower size limit down to (10 to 20) nm. These devices amplify the light scatter from the particle by condensing a vapor around it and growing the particle to a several micrometer (>> 1 μm) sized droplet, similar to the process that forms clouds in the atmosphere. The micrometer sized droplets are easily detected but the measurement is independent of the particle size, shape, and refractive index. Therefore the instrument gives a measure of particle occurrence or counts only.

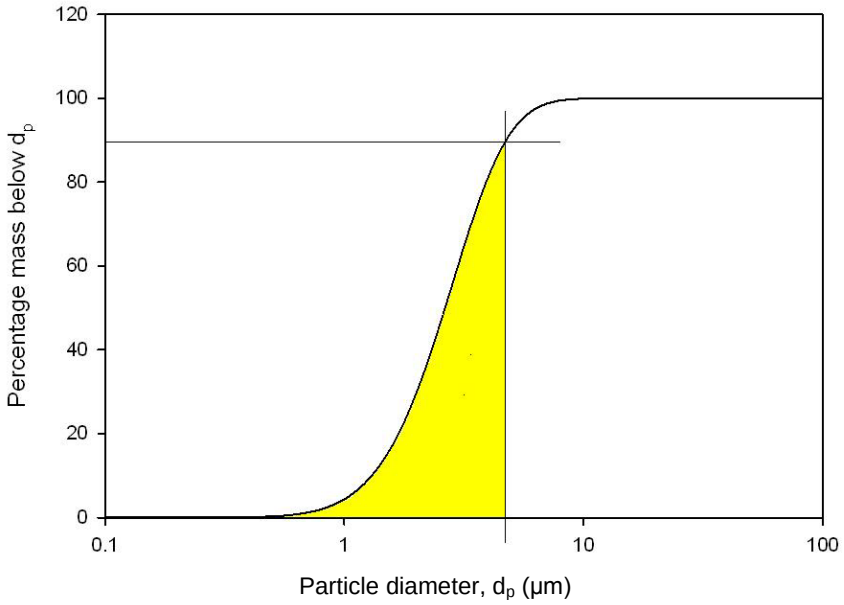

Figure 6 Cumulative mass distribution.

An important consideration for all instruments is the range of particle diameters they can measure. As will be seen, this feature can significantly affect their accuracy for certain aerosols, particularly in the determination of mass concentration. To illustrate this point, it is useful to refer to the cumulative mass distribution shown in Figure 6.

Figure 6 is best appreciated in comparison to the distributions shown in Figure 1 and Figure 3. In those cases the graphs of the PSD are presented, which describes the amount of mass contributed by a particle of a specific size. In contrast, the cumulative distribution seen in Figure 6 expresses the amount of mass contained from the smallest possible size (nominally a diameter of zero), up to a given diameter d_p. When d_p is equal to the largest size in the distribution, the cumulative distribution equals 100 percent by definition, as all the mass of all size particles has been accounted. In Figure 6, this occurs at approximately 10 μm. The yellow shaded area represents the value of d_p for which 90 percent of the mass in the distribution is accounted. In

this example, this occurs at a value of approximately 7 μm. More simply stated, 90 percent of the mass of the total distribution is contributed by particles 7 μm and smaller.

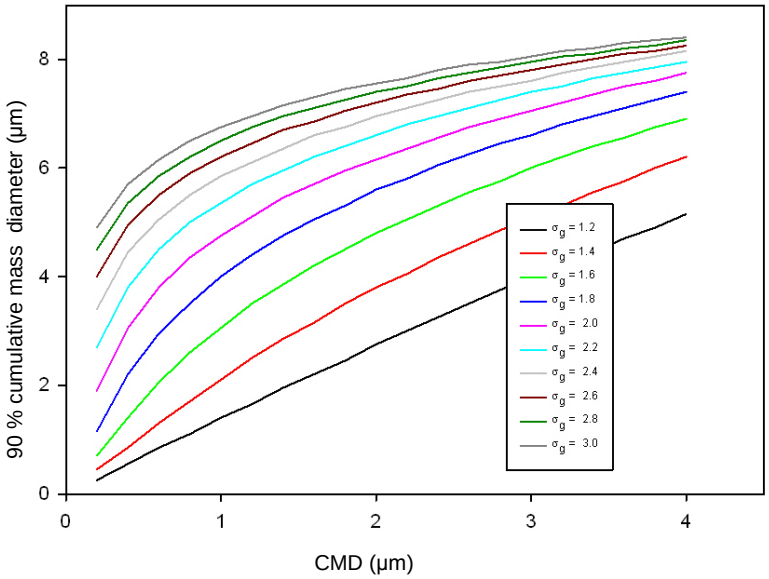

Figure 7 Diameters for 90 % cumulative mass for a range of respirable aerosols.

Illustrating the relationship of the cumulative mass and the particle size range afforded by a given measuring instrument is aided by Figure 7. The horizontal axis of the graph corresponds to the CMD of the distribution, and ranges from 0.2 μm to 4.0 μm. These values are reasonably typical for the aerosols under consideration. The vertical axis of the graph corresponds to the 90 % cumulative diameter. For the aerosol shown in Figure 6, for example, this diameter was roughly 7 μm as discussed above. A family of curves is shown for values of σ_g ranging from 1.2 to 3.0. This range of values is also typical for the types of aerosols of interest here. For any combination of CMD and σ_g throughout their respective ranges, Figure 7 indicates the particle diameter below which 90 % of the mass of the total distribution is found. It should be noted that the PSDs used to calculate the values seen in Figure 7 were first weighted with the curve shown in Figure 2. Specifically, Figure 7 shows the 90 % mass cumulative distribution for the respirable fraction of each aerosol under consideration.

Two extreme cases shown in Figure 7 help to illustrate how the accuracy of a given instrument is influenced by the size range of particles it can measure. Consider the case of CMD = 0.2 μm, and σ_g = 1.2. This point corresponds to the left-most end of the lowest curve in the graph. It can be seen for this distribution that 90 % of the total mass is contributed by particles smaller than roughly 0.2 μm. Consider the opposite extreme, where CMD = 4.0 μm and σ_g = 3.0. In this case, 90 % of the mass for this aerosol is contributed by particles roughly 8 μm and below.

For many handheld OPCs, the particle size upper limit is on the order of 4 μm to 5 μm. If 90 % of the total mass is contributed by particles as large as 8 μm as in the second example, such an

instrument would under report the total mass, since it is unable to measure the largest sizes that contribute to the cumulative mass.

In more practical terms, handheld OPCs are often more limited in this application by the smallest size particles that they can measure. This lower size limit is typically on the order of 0.3 μm to 0.5 μm. For the first example that was considered (CMD = 0.2 μm, and σ_g = 1.2), this represents an extremely significant consideration. Since 90 % of the cumulative mass occurs below this size, such instruments would grossly under report the total mass. In the extreme case, they would literally report nothing at all. In summary, Figure 7 illustrates that the range of particle sizes that a given instrument can detect significantly affects its accuracy depending upon the specific aerosol being measured.

An additional consideration in the use of OPCs concerns what are referred to as coincidence errors. While the above discussion has centered on the measurement of the mass of an aerosol, coincidence errors are related to the number of particles in the distribution. Functionally, an OPC measures one particle at a time. It is important to realize, however, that both the incoming beam of light that illuminates the particles, and the region of space that is viewed by the optical detector are not infinitesimally small points. Rather, the incident beam of light illuminates a certain volume of space (on the order of a cubic millimeter, typically). Similarly, the detector that measures the scattered light is sensitive to particles that reside in a certain spatial region. The overlap between these regions is referred to as the Optical Sample Volume (OSV). Specifically, a particle residing within the OSV scatters light from the illuminating beam, and this light is measured by the optical detector.

Since an OPC is used to measure the size of each particle in the aerosol individually, it is important that no more than one particle occupies the OSV at a time. If the number of particles in a given volume of aerosol is very, very low, there is a high probability that this will be true. However, if the number concentration is continuously increased, eventually there will be a large probability of more than one particle being in the OSV at the same time. When this occurs, the detector collects the scattered light from more than one particle. Referring to the example calibration table shown in Figure 5, it can be seen that the OPC erroneously interprets this event as arising from a single particle that is larger than the individual particles themselves. For this reason, an important performance characteristic for an OPC concerns the largest number concentration that it can safely measure without a significant probability for coincidence errors. This situation can be appreciated by referring to Figure 8:

The horizontal axes of Figure 8 depict the same range for CMD and σ_g as in Figure 7 above. The total mass concentration is fixed at a value of 3 mg/m^3; corresponding to the ACGIH exposure standard previously discussed. Similar to the calculation relating to Figure 7, the various distributions were weighted to provide only the respirable fraction. The vertical axis illustrates the number concentration corresponding to the values of CMD and σ_g for a given aerosol.

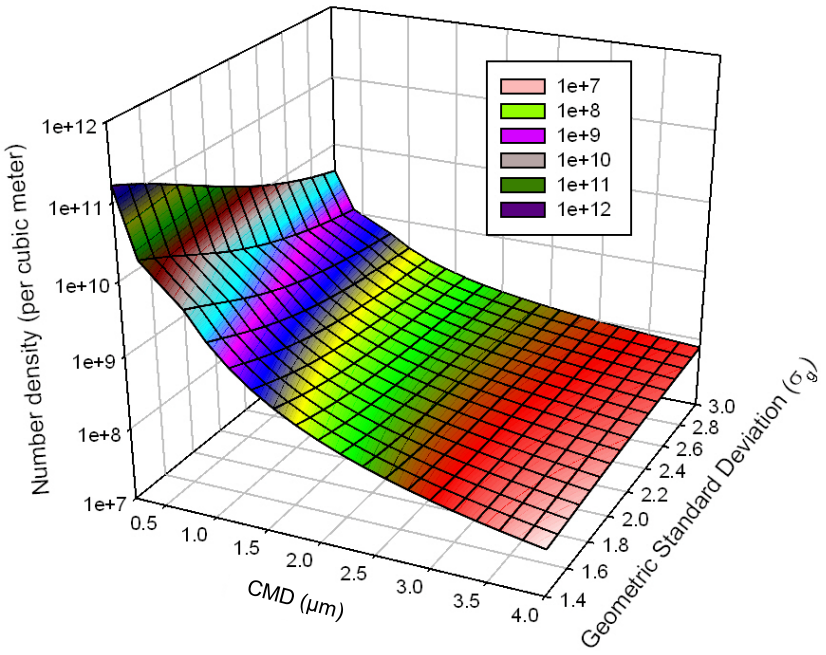

Figure 8 Aerosol number concentration for a fixed mass concentration of 3 mg/m3.

From Figure 8, it can be seen that the number density associated with these various aerosols varies significantly. Specifically, the lowest number density (CMD = 4.0 μm, σ_g = 1.4) and the highest (CMD = 0.2 μm, σ_g = 1.4) differ by almost four orders of magnitude. Of greater concern is that the highest number density case exceeds the value where many OPCs can operate without risk of coincidence errors. This figure illustrates potential difficulties in using OPCs when the properties of the PSD are not known in advance with any certainty. This situation can be further complicated if several materials, each with different PSDs, are present simultaneously.

In summary, several considerations have been identified that potentially affect the accuracy of OPCs in measuring aerosol mass exposure. These considerations must be reflected in the testing protocol used to evaluate the performance of individual instruments. A matrix of test aerosols and conditions must be specified to address the following factors that have been identified in the preceding discussion:

1. Since OPCs nominally measure particle size, uncertainty in the particle density gives rise to a proportional uncertainty in determining the measured mass exposure. Individual instruments may include provisions for inputting the particle density, while in other cases a default value is assumed. This aspect must be further investigated and quantified for aerosols or combinations of aerosols for which the density is not well known.

2. The measurement of particle size is affected by the particle refractive index. Some instruments are calibrated for a number of particle materials, where in other cases a default value is assumed. For this reason, a range of aerosols with differing values of refractive index must be examined. These tests must also address combinations of materials where the

individual refractive indices may not be well known, or where the relative amounts of the individual materials may be unknown.

3. The range of particle sizes that a specific OPC can measure can significantly affect the accuracy in determining mass concentration. Test aerosols and combinations of aerosols can be used to address this consideration by virtue of having an appropriately wide range of PSDs.

4. Coincidence errors arise when the number density of the aerosol becomes sufficiently large. For some OPCs, this can occur at number concentrations that are less than the corresponding allowable mass exposures. It is important that the concentration of test aerosols with a range of PSDs be varied to determine when this performance limit is reached for individual instruments.

EXPERIMENTAL METHODS

Apparatus

A major challenge in sampling particulates is ensuring that the instrumentation is not over exposed or saturated with too many particles. Saturation can lead to the coincidence errors mentioned previously. Frequent saturation can lead to long term measurement error from optics degradation due to particulates depositing on the optics. This situation requires cleaning, maintenance, and possible recalibration. Therefore, sampling from environments with high loadings of particulates requires dilution of the sample stream.

In this study, particulate sampling occurs very near the source and within a closed system. The dilution that would normally occur in an open system is absent and therefore the particle loading is often beyond the limits of some of the instrumentation. A custom sampling system with multiple levels of dilution was designed for this study. Because OPCs, in general, have lower concentration limits than dust monitors, multiple stages of dilution were required in order to measure particle number concentration and particle mass concentration simultaneously.

The smoke or aerosol sample was drawn from a mostly homogenous mixture of air and particulates. A schematic of the sample system, Figure 9, demonstrates that the sample was diluted twice before passing through an enclosure that held the dust monitors, and then it was diluted twice more before passing through a cell from which the particle counters would draw their sample. Stage 1 of the dilution occurred at the venturi pump which drew the sample from the source. A stream of filtered air was added just after the venturi pump for the second stage of dilution. The third and fourth stages of the dilution were achieved by partitioning a desired amount of the sample with laminar flow elements and passing the remainder through HEPA filters to remove the particulates before reintroducing it back into the sample stream. A photograph of the system is shown in Figure 10. The system was capable of achieving a dilution ratio of 5000:1. The typical range of dilution ratios used in this study is shown in Figure 11 as the area filled with hash marks.

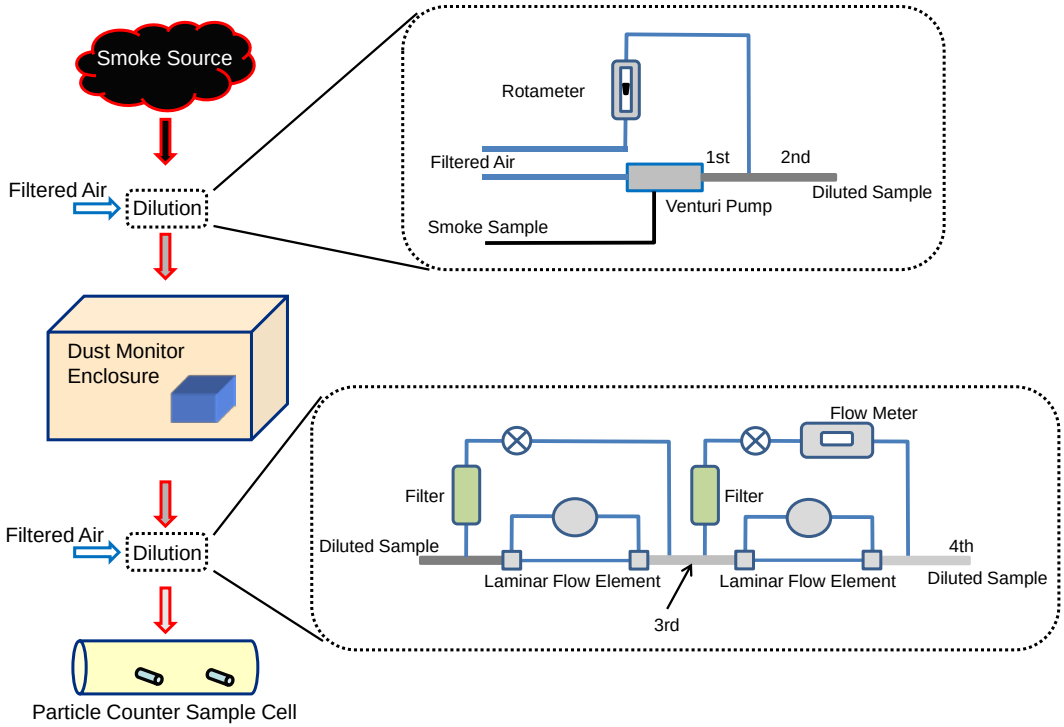

Figure 9 Schematic of the sampling system demonstrating the multiple stages (1st, 2nd, 3rd, 4th) of dilution.

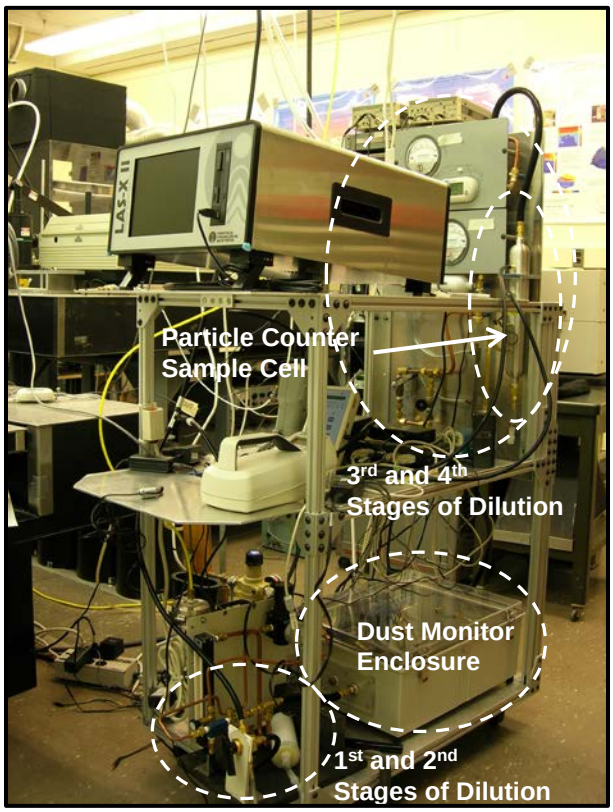

Figure 10 Photograph of sampling system.

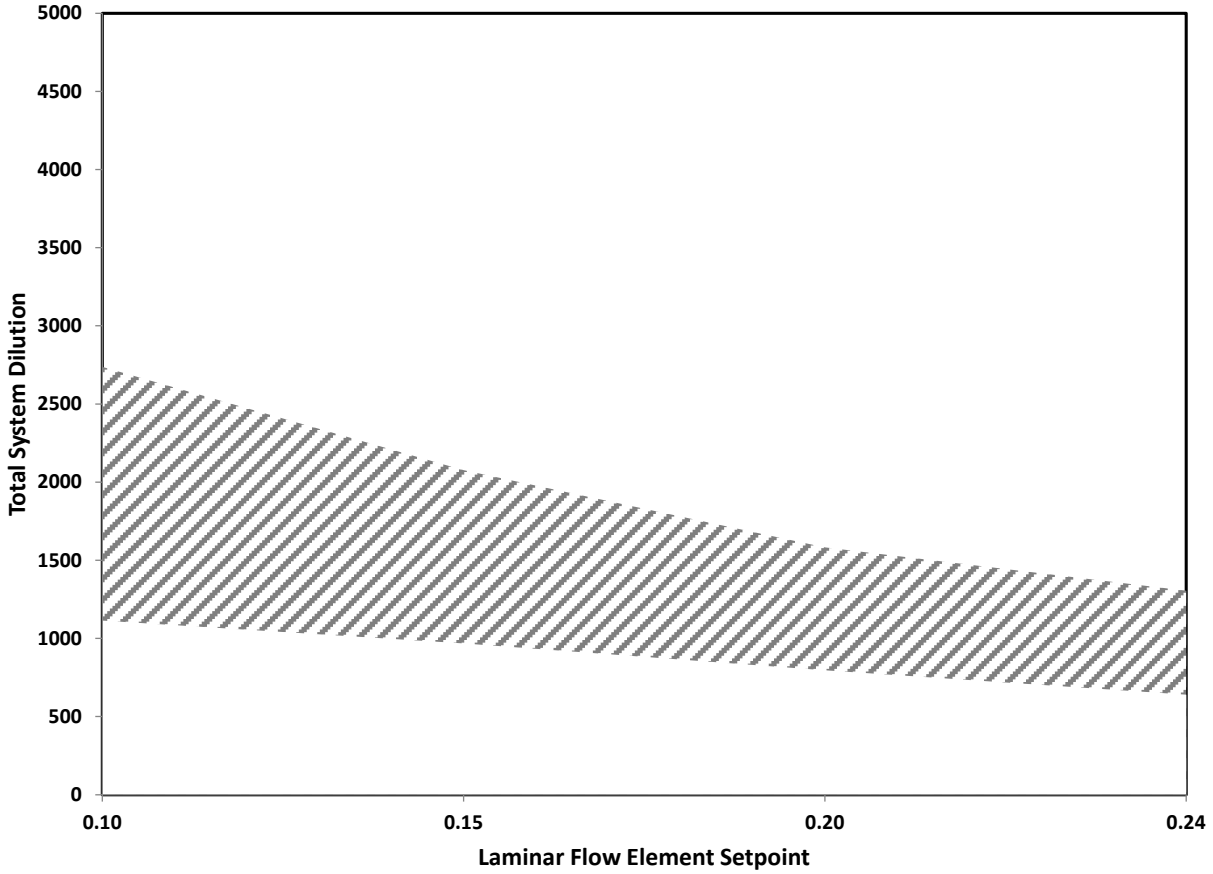

Figure 11 Range of dilution ratios used for this study.

When sampling combustion generated particulates, typically the gas sample will be heated to preserve the condition of the sampled particulates as they are transported through the sampling system and to the detector. For the objective of these experiments, simulating real smoke particles that are representative of the fire overhaul environment, heating the air sample is not necessary. When overhaul begins, the combustion products have been diluted significantly by the ambient air and they are significantly cooler than during the period of active fire. Therefore, by not heating the sample, the process is more reflective of the overhaul environment.

Measurements of particle count and particle size were conducted in order to provide reference information on particle concentration and size distribution. The samples for these measurements were drawn from the Particle Counter Sample Cell, where dilution was the highest. Particle concentration was measured using a CPC (Kanomax Model 3800), while the particle size distribution was measured using a particle size spectrometer with a range of 90 nm to 10,000 nm. (Particle Measuring Systems, Model LAS-X II). Manufacturer quoted expanded uncertainty (95 % confidence interval) for the CPC was ±20 % of the measured particle concentration. The quoted expanded uncertainty for measurement of particle size was ±6 % for the particle spectrometer. The CPC provides a reference measurement that is independent of particle characteristics. It is a measure of particle occurrence.

Aerosols such as mineral oil (CMD=0.2 μm) and an aqueous glycol solution (theatrical fog, particle size range: 0.25 μm to 60 μm) were selected as surrogates for the particulates generated during overhaul. White (clear) mineral oil has been used to test smoke detectors and is a reasonable surrogate for the particulates generated during the material pyrolysis prior to flame ignition. A smoke detector tester (Gemini 501) was used to generate mineral oil droplets. Similarly, glycol fog served as a surrogate for particulates generated during pyrolysis. A theatrical fog machine (Rosco 1700) was used to aerosolize the aqueous glycol solution. Each aerosol was used to evaluate the response of the dust monitors under controlled experimental conditions.

Several materials were selected to represent the sources of particulates generated during a fire and firefighting activities in building, Table 1. Wood materials like cedar, plywood, oriented strand board (OSB), and pine were selected as representative building materials. Similarly, gypsum board was selected as a representative building material. Cotton upholstery and polyurethane foam represent the material make-up of furniture items. Some of the wood materials may also be included in this category.

Table 1 Material dimensions and mass.

Material	Length (cm)	Width (cm)	Thickness (cm)	Mass (g)
Cedar	10.0	10.0	2.6	121.7
Plywood	10.1	10.1	1.5	106.4
OSB	10.1	10.1	1.2	80.6
White Pine	10.1	10.1	1.9	84.3
Gypsum Board	9.8	9.8	1.3	69.7
Cotton Upholstery*	10.0	10.0	0.3	12.3
PU Foam	10.0	10.0	2.5	6.6

* Folded sheet with layer thickness of 0.17 cm.

The material samples were cut into squares, approximately 10 cm x 10 cm, for burning in the cone calorimeter, a standard test apparatus used to determine the heat and smoke contribution to a fire from test materials. Sample conditioning and burning followed the procedures of ASTM E 1354-11a. [11] Each sample was placed in the cone calorimeter (horizontal orientation) and exposed to a heat flux of 25 kW/m^2 from the radiant cone to induce pyrolysis and subsequent burning of the sample. The samples were exposed until the fire and all visible radiation from the sample, i.e. glowing, had ceased. During sample exposure, the dilution system was used to collect aerosol samples from the exhaust of the cone calorimeter.

RESULTS AND DISCUSSION

Response to smoke surrogates

Four optical dust monitors were simultaneously exposed to the smoke surrogates (aerosolized mineral oil and an aerosolized aqueous glycol solution) to characterize their response. The dust monitors were selected to be representative of those available on the market and are here identified by the letters A, B, C, and D. Each dust monitor is a handheld device and was marketed as a personal exposure monitor. Instruments A, B, and C were active sampling devices, meaning they were equipped with an internal pump to continuously extract a sample of air from the surrounding environment. Instrument D was not equipped with an internal pump and therefore performed a passive sample of the surrounding environment. Each of the instruments inferred mass concentration from the laser light scattered off the particles in the sampling volume. Measurements of particle count concentration were conducted simultaneously using the CPC. These measurements were from a diluted sample in order to avoid coincidence errors for the CPC. Each dust monitor was operated using its default or factory setup; therefore measurements present here are for the factory calibration of each instrument. Manufacturer quoted relative expanded uncertainty estimates were ±15 %, ±5 %, ±10 %, and ±10 %, for instruments A, B, C, and D, respectively.

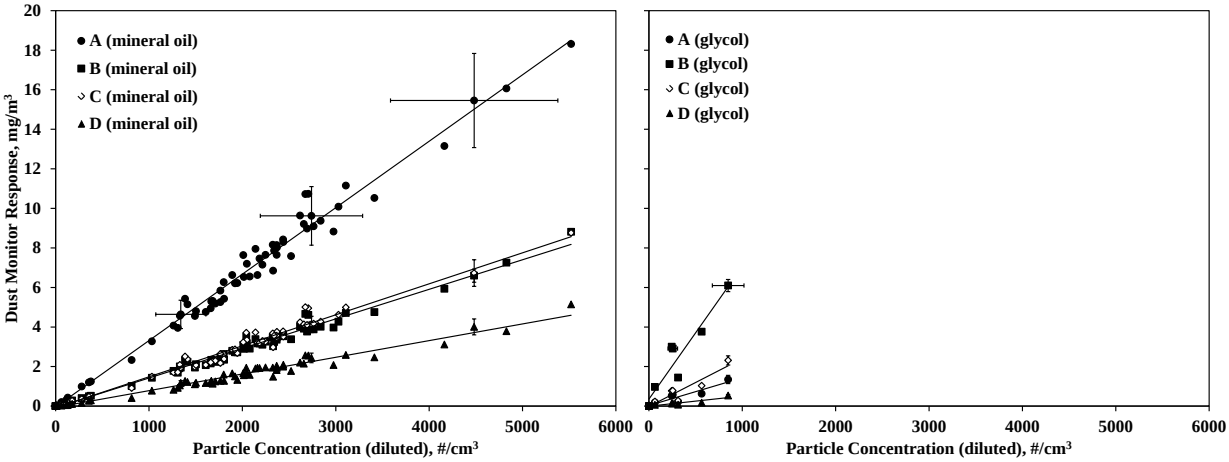

Figure 12 Dust monitor response to the number concentration (diluted) of smoke surrogates.

Dust monitor mass concentration measurements are plotted with respect to CPC particle count concentration measurements in Figure 12. As expected, the response of the dust monitors was linear. Most important, the response was linear over the range of mass concentration defined by the ACGIH exposure limits for particulates, 3 mg/m^3 for respirable particulates and 10 mg/m^3 for inhalable particulates. The factory calibration for each dust monitor is referenced to a gravimetric measurement of the industry standard material, aerosolized fine test dust (ISO 12103-1, A2), either by direct comparison to the gravimetric measurement or a reference instrument with direct comparison to the gravimetric measurement. For aerosolized mineral oil, instrument A had the greatest response to particle count concentration, followed by instruments C and B which had similar responses. Instrument D had the lowest response; a factor of 2 lower than instruments B and C and a factor of 4 lower than instrument A. Three of the instruments logged significantly different values for particle mass concentration for the aqueous glycol solution, while two responded with similar outputs. The variation in instrument response for the

same aerosol demonstrates the large uncertainty associated with using these instruments in their factory configuration to detect an aerosol other than the calibrating aerosol. However, the linear response of the instruments demonstrates that they can be calibrated for the aerosol of interest.

The CPC response is independent of the physical characteristics of the particulates. Figure 12 captures the response of the dust monitors to a change in the physical characteristics of the particulates. The aerosolized mineral oil and aqueous glycol solution are both liquid droplets, but with differences in size distribution and refractive index (mineral oil: n=1.47; aqueous glycol solution: $1.33 \leq n \leq 1.45$). The response of the dust monitors to particle count concentration of the aqueous glycol solution is different when compared to that of the mineral oil. Instrument D again had the lowest response, and decreased by almost a factor of 2 when compared to mineral oil. Instrument B had the greatest response and increased by a factor of 5 when compared to mineral oil. The change in ranking of the dust monitor response between mineral oil and glycol follows: Mineral Oil – A; C; B; D; Glycol – B; C; A; D. This change in response for smoke surrogates or liquid droplet aerosols demonstrates the need for an aerosol or mixture of aerosols representative of the fire overhaul environment. However, there is a wide variety of aerosols in fire overhaul, so finding a single representative aerosol may prove difficult.

Response to Burning Materials

Material samples were burned in the cone calorimeter (see Figure 13) and the instruments were exposed to the products of the burning materials in order to characterize their response to real smoke samples. Using the sampling system described earlier, air samples were drawn from the exhaust of the cone calorimeter and diluted with filtered air before being simultaneously sampled by each of the instruments: four handheld dust monitors (labeled A through D), the CPC, and the particle size spectrometer. This simultaneous sampling allowed a time history of each instrument's response to be recorded and correlated to specific events during the burning process. A standard output of the cone calorimeter is the time history of the heat release rate for the burning material which could also be correlated to specific events. Events identified during the cone burns by visual observation were: ignition, flaming, and flame-out. Pyrolysis occurs just prior to ignition and an afterglow follows the flame-out. Time history plots of heat release rate, particle mass concentration, particle number concentration, and particle count median diameter (CMD) are presented in the following sections. Particle CMD was computed from the measured particle size distribution (PSD), assuming a lognormal distribution, equation 3.

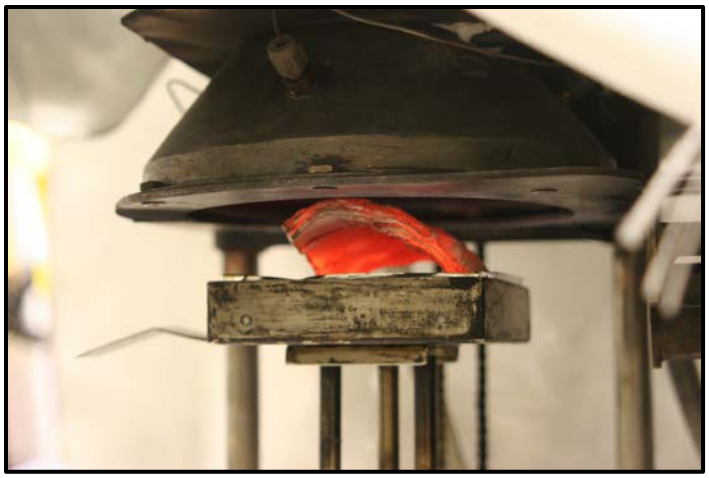

Figure 13 Photo of glowing OSB sample in the cone calorimeter after the flame has extinguished.

Cedar

Samples were cut from cedar planks and an example of the sample before burning is shown in the photo in Figure 14. Four samples were burned in the cone calorimeter to generate repeat experiments. The residual was a block of wood char also shown in Figure 14.

Figure 14 Photo of cedar samples before and after being burned in the cone calorimeter.

Figure 15 is a representative display for the time history of heat release rate, particle mass concentration, particle number concentration, and particle CMD, resulting from the burning of a single cedar sample. Prior to ignition, during pyrolysis, the measured heat release rate was negligible. After ignition of the cedar sample, during flaming, the measured heat release transitioned through a sharp initial peak and then remained relatively steady for a period. Later it transitioned through another wider and lower magnitude peak. After that transition the flame extinguished (flame-out) and the heat release dropped during the period of afterglow.

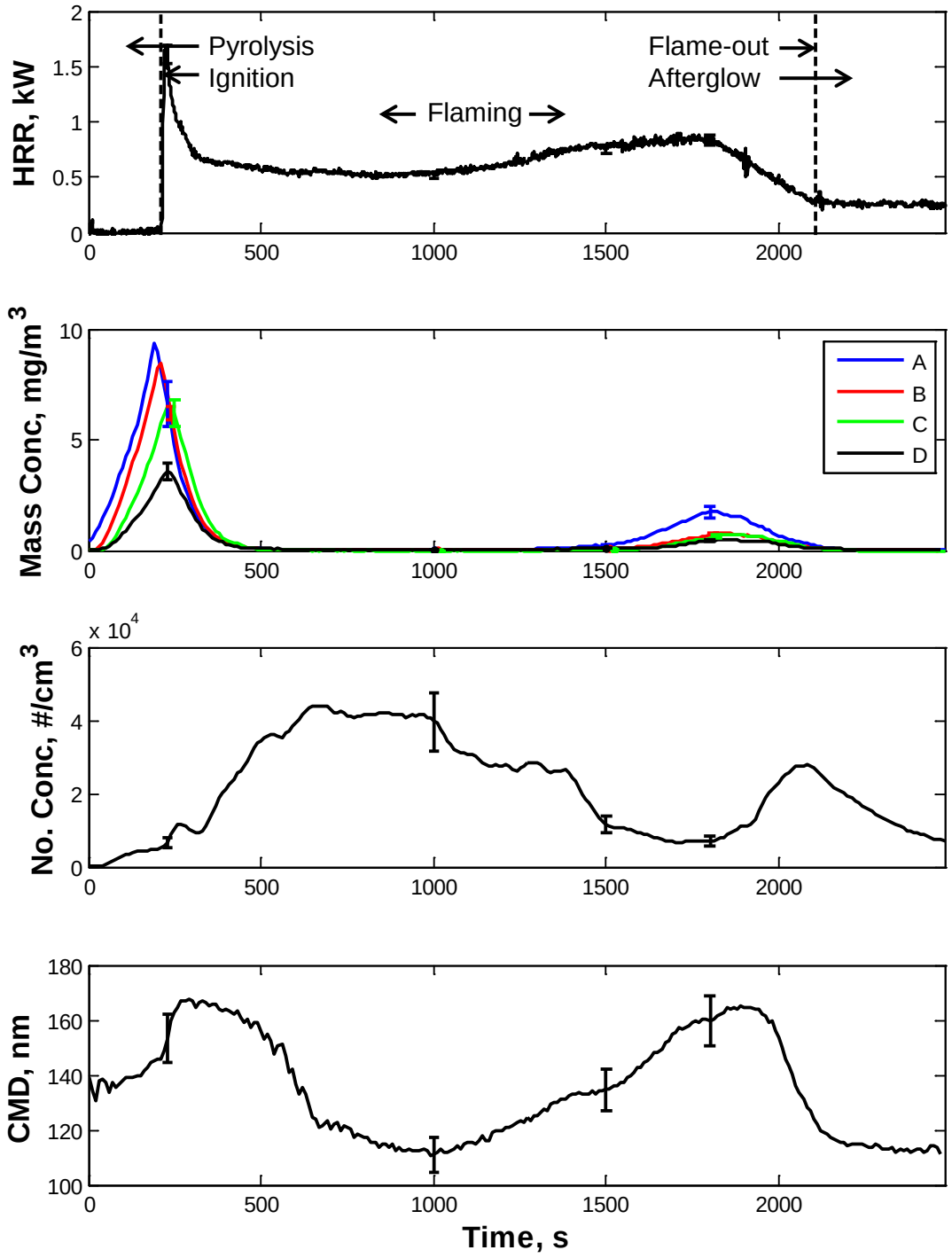

Figure 15 Time history measurements of heat release rate, particle mass concentration (diluted), particle number concentration (diluted), and particle count median diameter for a burning cedar sample. Cone calorimeter incident heat flux was 25 kW/m^2.

The handheld detectors measured two peak periods of particle mass concentration generated by the burning cedar sample. The first occurred during a period overlapping the pyrolysis and ignition of the sample. This also correlated with the first peak of heat release rate. The second peak in mass concentration was wider, much smaller in magnitude, and occurred near the second peak of heat release rate, just prior to the flame extinguishing. The measured mass concentration was negligible during the majority of the flaming period and during the period of afterglow.

The CPC measured the particle number concentration generated by the burning cedar sample. Measured particle number concentration was largest during the flaming period and between the two peaks of heat release rate. When the measured number concentration was large the measured mass concentration was low, if not negligible. Peaks in CMD correlated with peak mass concentration, while periods of lower CMD values correlated with periods of high number concentration. These observations suggest that a large fraction of the particles generated during the flaming period did not generate significant optical scattering in the dust monitors because they were either too small, of low refractive index, or both.

Plywood

Samples were cut from plywood sheet and an example of the sample before burning is shown in the photo in Figure 16. Five samples were burned in the cone calorimeter to generate repeat experiments. The residual was a block of wood char also shown in Figure 16.

Figure 16 Photo of plywood samples before and after being burned in the cone calorimeter.

Figure 17 is a representative display for the time history of heat release rate, particle mass concentration, particle number concentration, and particle CMD, resulting from the burning of a single plywood sample. Prior to ignition, during pyrolysis, the measured heat release rate was negligible. After ignition of the plywood sample, during flaming, the measured heat release increased sharply and went through a gradual peak. The heat release rate then remained relatively steady for a period. Later it transitioned through another gradual peak of greater width and magnitude. The heat release rate then dropped off and remained relatively steady for the remainder of the burn.

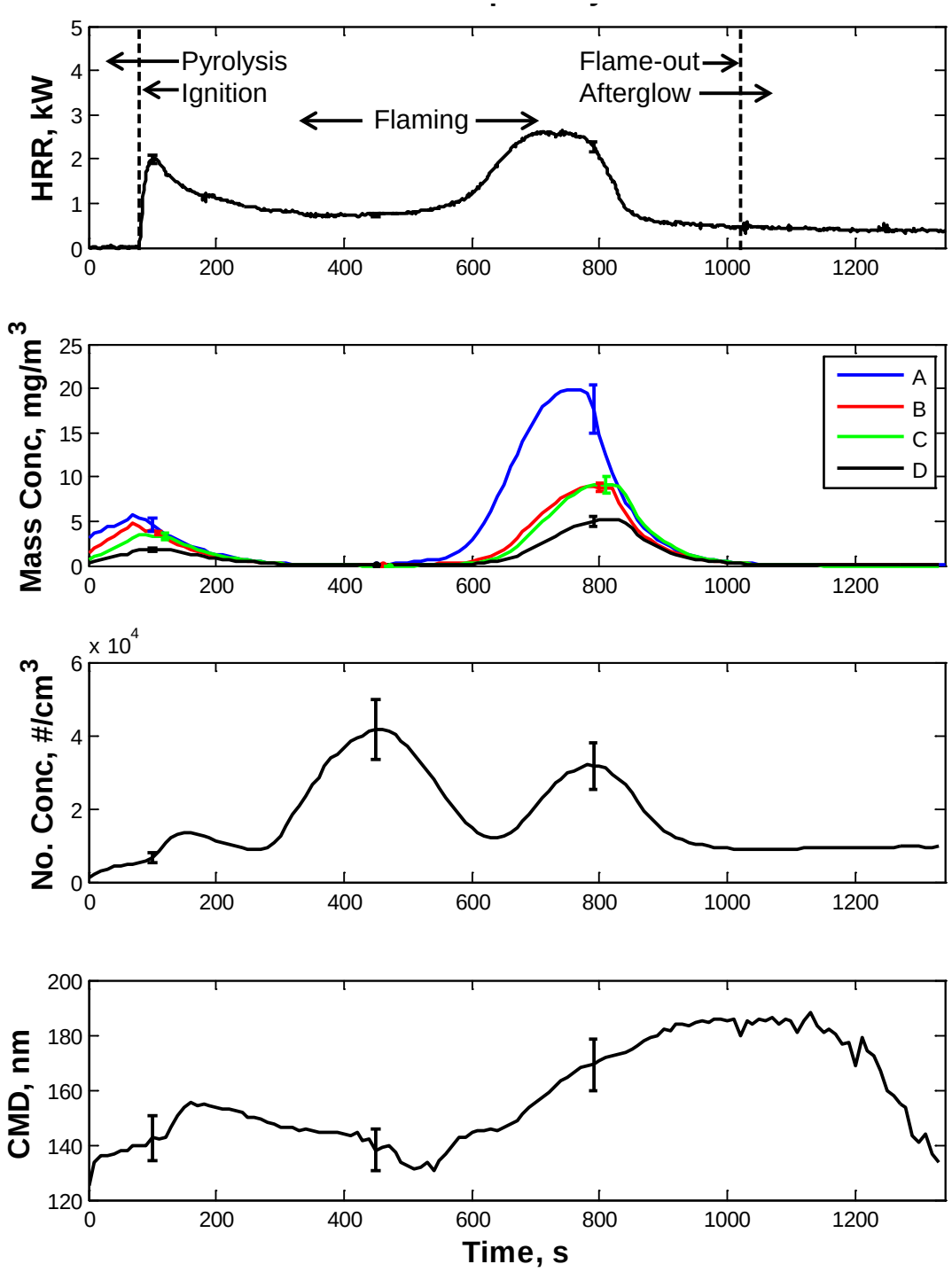

Figure 17 Time history measurements of heat release rate, mass concentration (diluted), number concentration (diluted), and count median diameter for a plywood sample. Cone calorimeter incident heat flux was 25 kW/m^2.

The handheld mass concentration detectors measured two peak periods that correlated with the peaks of heat release rate. The first occurred during a period overlapping the pyrolysis and ignition of the sample and was the minor of the two. The second peak was significantly greater than the first in magnitude but similar in width. It occurred during the second peak of heat release rate. With the exception of the peak regions, the measured mass concentration was generally very low.

The CPC measured significant particle number concentration during the plywood sample burn. For three of the five samples burned, the peak number concentration was measured during the flaming period and between the peaks observed in the particle mass concentration trace. A secondary peak of number concentration was observed near the end of the flaming period during the second heat release rate peak. Similar to the cedar sample, when the measured number concentration was at its largest value the measured mass concentration was at its lowest. This observation again suggests that a large fraction of the particles generated during flaming did not generate sufficient optical scattering in the dust monitors. In general, the CMD went through two local peaks during the burn, with the second peak having the greatest magnitude.

Oriented Strand Board (OSB)
Samples were cut from a sheet of OSB and an example of the sample before burning is shown in the photo in Figure 18 Four samples were burned in the cone calorimeter to generate repeat experiments. The residual was a block of wood char also shown in Figure 18.

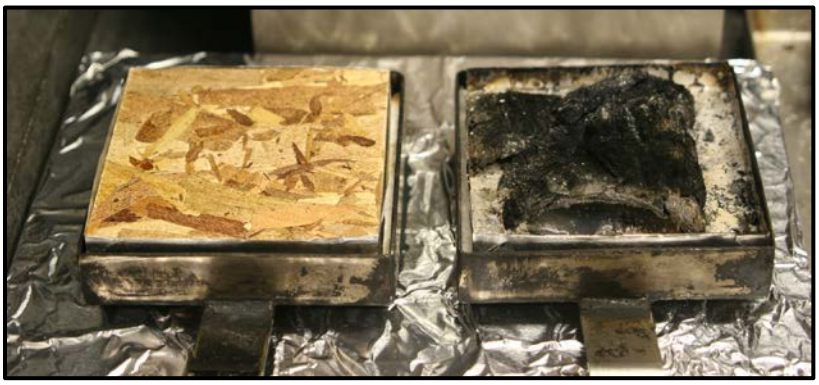

Figure 18 Photo of OSB samples before and after being burned in the cone calorimeter.

Figure 19 is a representative display for the time history of heat release rate, particle mass concentration, particle number concentration, and particle CMD, resulting from the burning of a single OSB sample. The general observations in the time history curves are almost identical to those of the plywood samples, with the exception of the particle number concentration trace. The difference is the absence of the peak number concentration during the flaming period and between the two heat release rate peaks. The remaining peak number concentration correlates with the peak mass concentration.

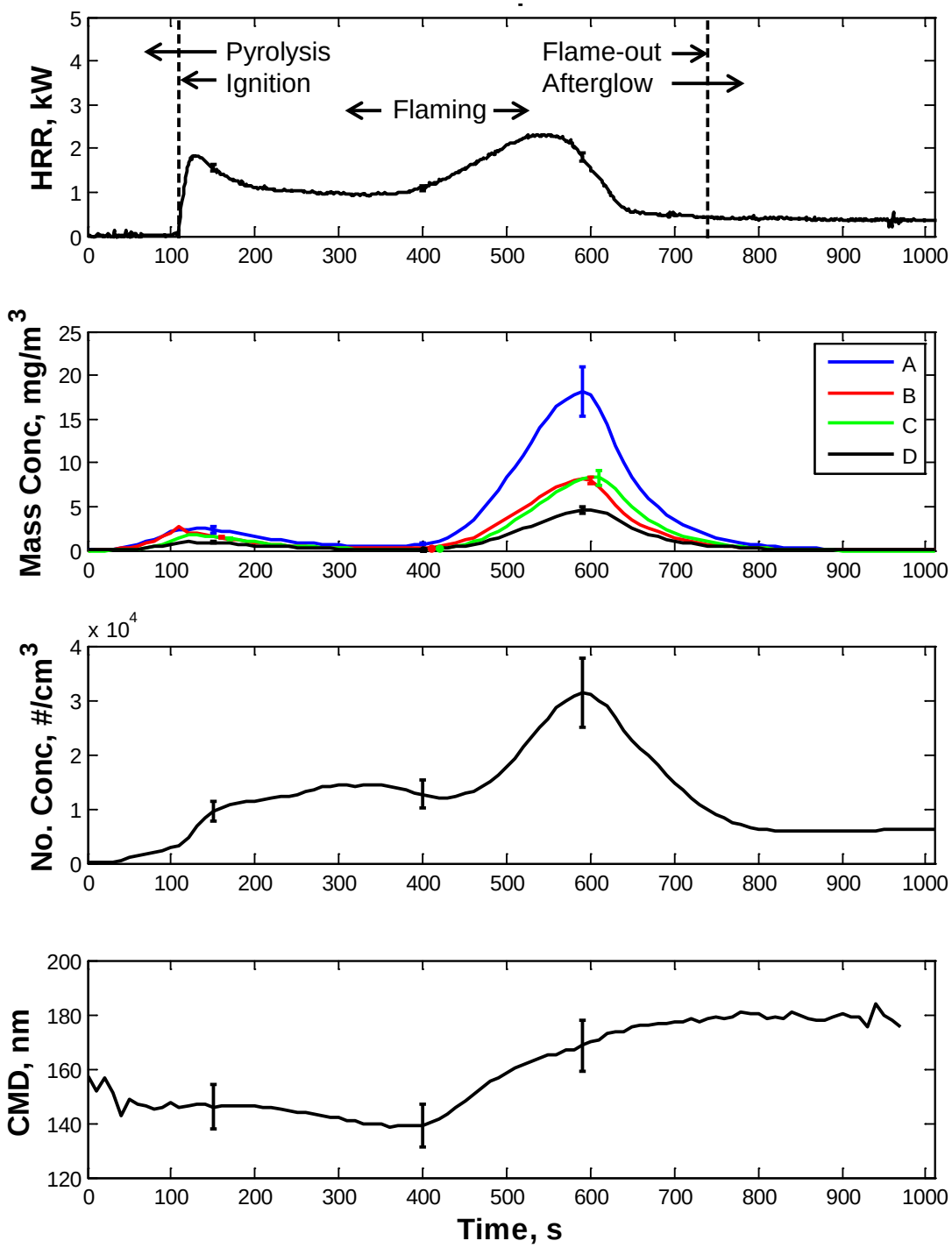

Figure 19 Time history measurements of heat release rate, mass concentration (diluted), number concentration (diluted), and count median diameter for an OSB sample. Cone calorimeter incident heat flux was 25 kW/m^2.

Pine

Samples were cut from planks of pine and an example of the sample before burning is shown in the photo in Figure 20. Four samples were burned in the cone calorimeter to generate repeat experiments. The residual was a block of wood char also shown in Figure 20.

Figure 20 Photo of pine samples before and after being burned in the cone calorimeter.

Figure 21 is a representative display for the time history of heat release rate, particle mass concentration, particle number concentration, and particle CMD, resulting from the burning of a single pine sample. In general, the burning pine sample has two distinct peaks of heat release rate; the first being a very narrow peak occurring right after ignition, and the second being a more broad peak occurring just prior to the flame extinguishing. The magnitude of both peaks is very similar, but in general the first peak is the greatest.

The handheld detectors measured two peak periods of particle mass concentration that correlated with the heat release rate peaks. The first peak was generally of larger magnitude, while both peaks had similar width. Measureable mass concentration, but significantly lower than the peak concentrations, was observed during the flaming period and between the two peaks. It was during this flaming period that the particle number concentration measured by the CPC was largest. Peaks in CMD correlated with peak mass concentration, while periods of low CMD values correlated with periods of high number concentration. These observations are similar to those of the cedar samples and suggest that a large fraction of the particles generated during this period of flaming did not result in in significant light scatter in the dust monitors.

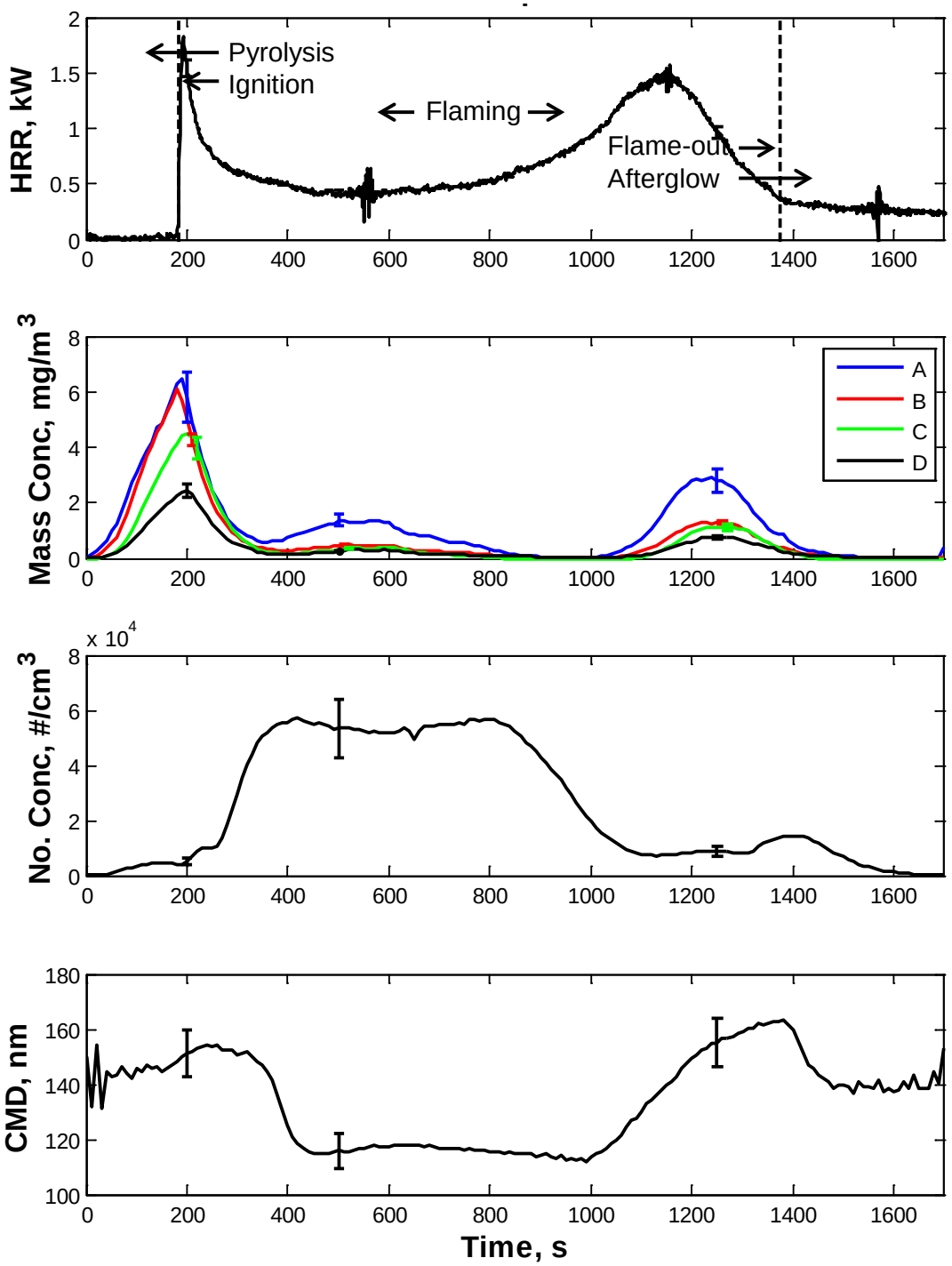

Figure 21 Time history measurements of heat release rate, mass concentration (diluted), number concentration (diluted), and count median diameter a for pine sample. Cone calorimeter incident heat flux was 25 kW/m^2.

Gypsum Board (Drywall)
Samples were cut from a sheet of gypsum board and an example of the sample before burning is shown in the photo in Figure 22. Four samples were burned in the cone calorimeter to generate repeat experiments. The residual was the charred paper covering and remaining gypsum shown in Figure 22.

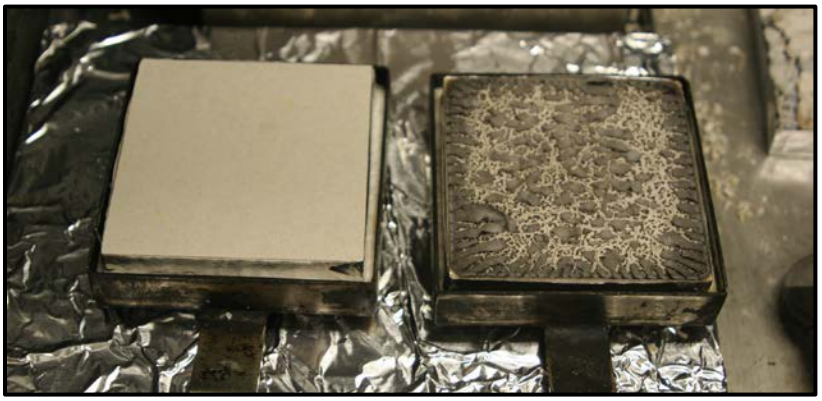

Figure 22 Photo of gypsum board samples before and after being burned in the cone calorimeter.

Figure 23 is a representative display for the time history of heat release rate, particle mass concentration, particle number concentration, and particle CMD, resulting from the burning of a single gypsum sample. The gypsum sample never ignited to form a flame. Its overall heat release rate was small compared to the other materials but it did generate a distinct peak. Distinct peaks were observed for the measured particle mass concentration and number concentration. Both occurred near the heat release rate peak. In general the peak mass concentration was to the left of the peak heat release rate while the peak number concentration was to the right. The CMD was relatively constant during the burn but a local maximum value was generally observed near the other peaks.

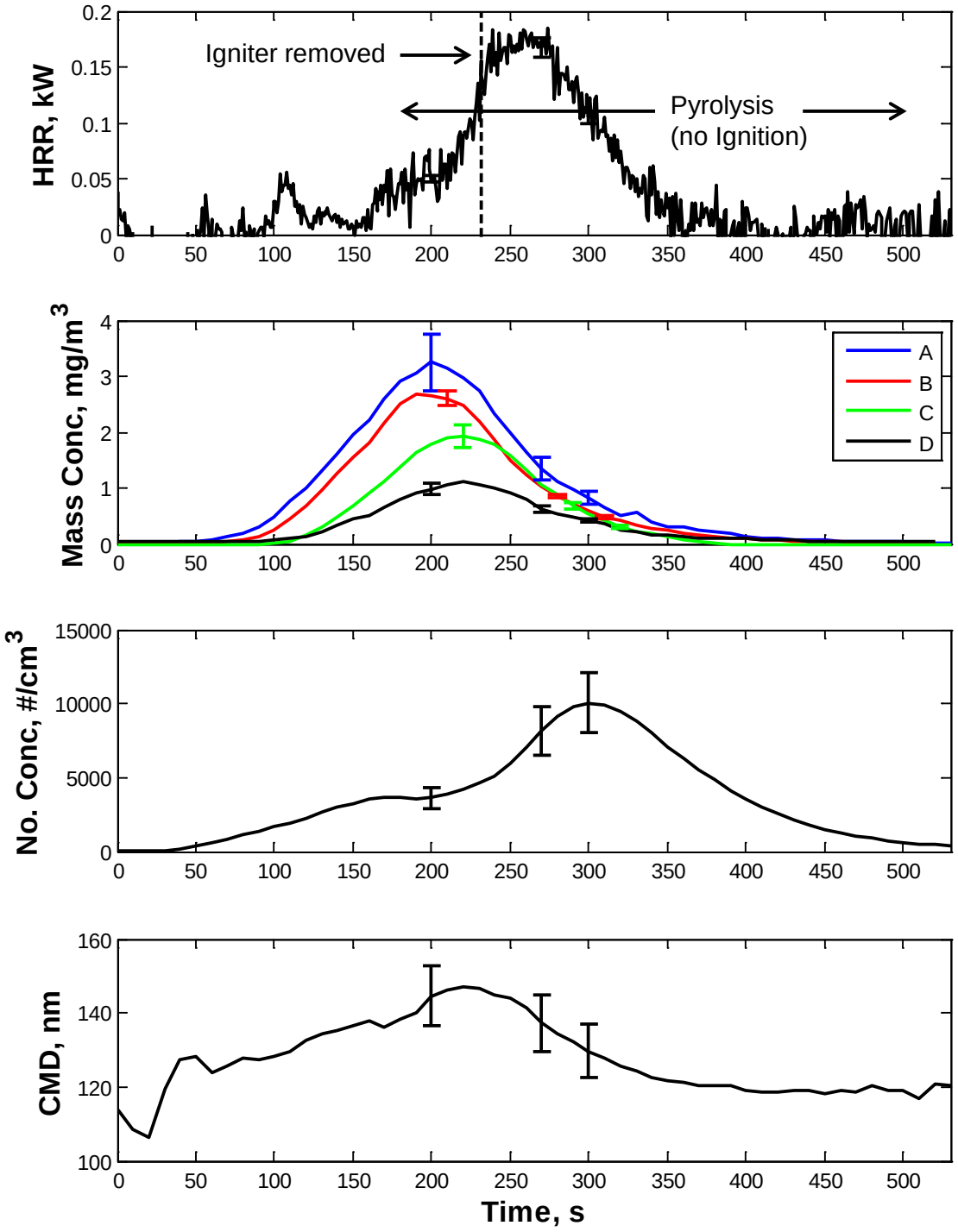

Figure 23 Time history measurements of heat release rate, mass concentration (diluted), number concentration (diluted), and count median diameter for a gypsum board (drywall) sample. Cone calorimeter incident heat flux was 25 kW/m^2.

Cotton Upholstery

Samples were cut from a sheet of cotton upholstery. The samples were cut to 20 cm x 10 cm and folded over once to have a final dimension of 10 cm x 10 cm. An example of the sample before burning is shown in the photo in Figure 24. Five samples were burned in the cone calorimeter to generate repeat experiments. The residual was the charred structure of the fabric shown in Figure 24.

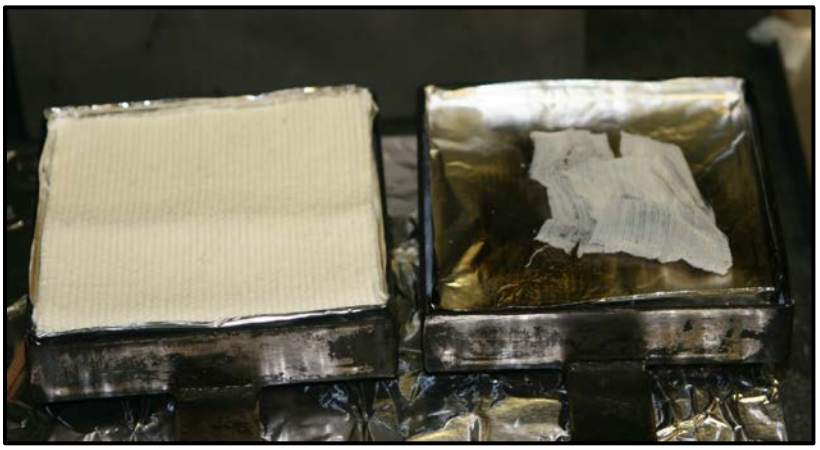

Figure 24 Photo of cotton upholstery samples before and after being burned in the cone calorimeter.

Figure 25 is a representative display for the time history of heat release rate, particle mass concentration, particle number concentration, and particle CMD, resulting from the burning of a single cotton upholstery sample. The flaming period for cotton samples is short compared to the wood products. A single peak transition of heat release rate was observed over this period. Distinct peaks were observed for the measured particle mass concentration and number concentration. Both correlated to the heat release rate peak, occurring near the heat release rate peak and slightly to the right or left. The CMD typically went through a local maximum near the other peaks and then was relatively constant during the remainder of the burn.

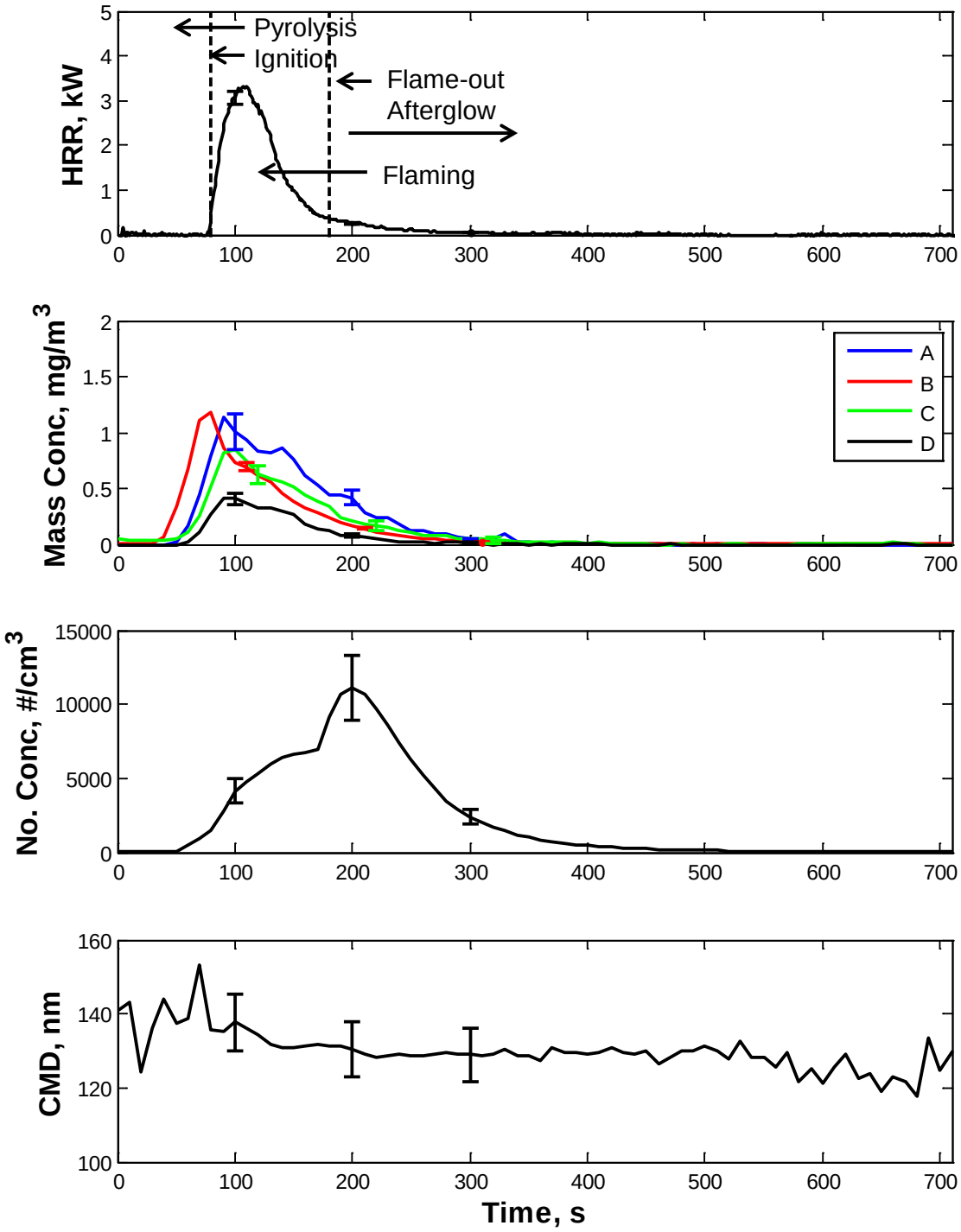

Figure 25 Time history measurements of heat release rate, mass concentration (diluted), number concentration (diluted), and count median diameter for a cotton upholstery sample. Cone calorimeter incident heat flux was 25 kW/m^2.

Polyurethane Foam

Samples were cut from a block of foam and an example of the sample before burning is shown in the photo in Figure 26. Four samples were burned in the cone calorimeter to generate repeat experiments. The residual char left after the foam melted and burned is shown in Figure 26.

Figure 26 Photo of polyurethane foam samples before and after being burned in the cone calorimeter.

Figure 27 is a representative display for the time history of heat release rate, particle mass concentration, particle number concentration, and particle CMD, resulting from the burning of a single foam sample. Like cotton, the flaming period for the polyurethane foam samples was short compared to the wood products. Also similar to the cotton samples, single peak transitions of heat release rate, particle mass concentration and particle number concentration were observed over this period. The distinct peaks were all correlated, occurring very close together. The CMD typically went through a step transition from a lower to higher value and then was relatively constant during remainder of the burn.

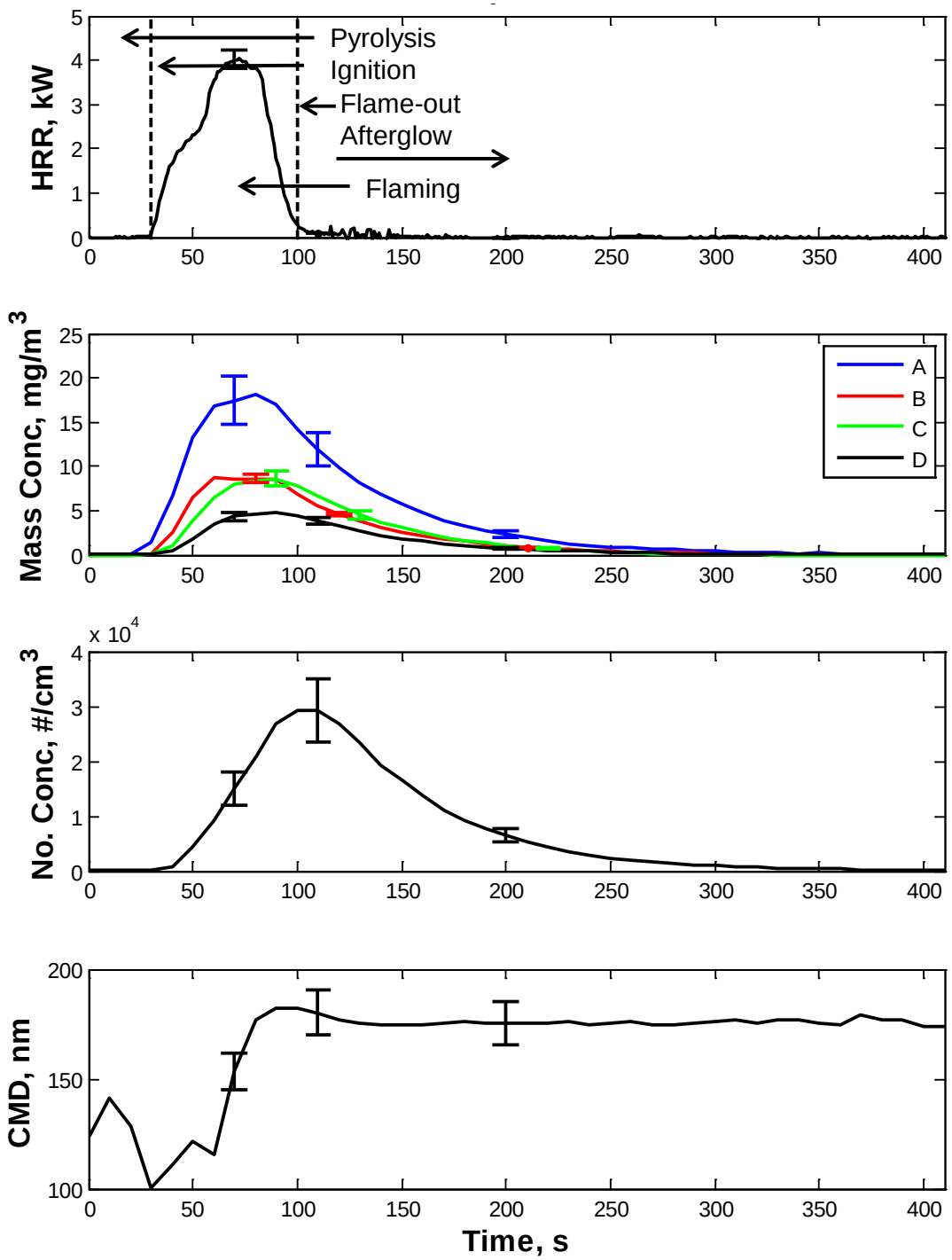

Figure 27 Time history measurements of heat release rate, mass concentration (diluted), number concentration (diluted), and count median diameter for a polyurethane foam sample. Cone calorimeter incident heat flux was 25 kW/m^2.

The time averaged particle mass concentration, particle number concentration, and particle CMD was computed for the duration of each burn (pyrolysis – ignition – flaming - flame-out - afterglow) for each of the seven materials considered here. Figure 28 displays the sample average and standard deviation of the repeat experiments for each material. When all of the materials are viewed together, there is not a clear correlation between mass concentration and number concentration as observed with the surrogate smokes. The response of each handheld dust monitor appears to be unique for each material. However, the response appears to be grouped among types of materials, for example fabrics and paper, polymers and engineered materials, and untreated wood products. The ranking of the sensitivity of the dust monitors was generally the same for each material. Instrument A had the greatest sensitivity, followed by instruments B, C, and D, in decreasing order. The same ranking was observed with the aerosolized mineral oil. Also, as observed with the mineral oil, the sensitivities of instruments B and C were generally equal. This suggests that aerosolized mineral oil may be a good candidate as a surrogate smoke. This type of data can be used to begin to understand how to rescale the factory calibrations for smoke particulates.

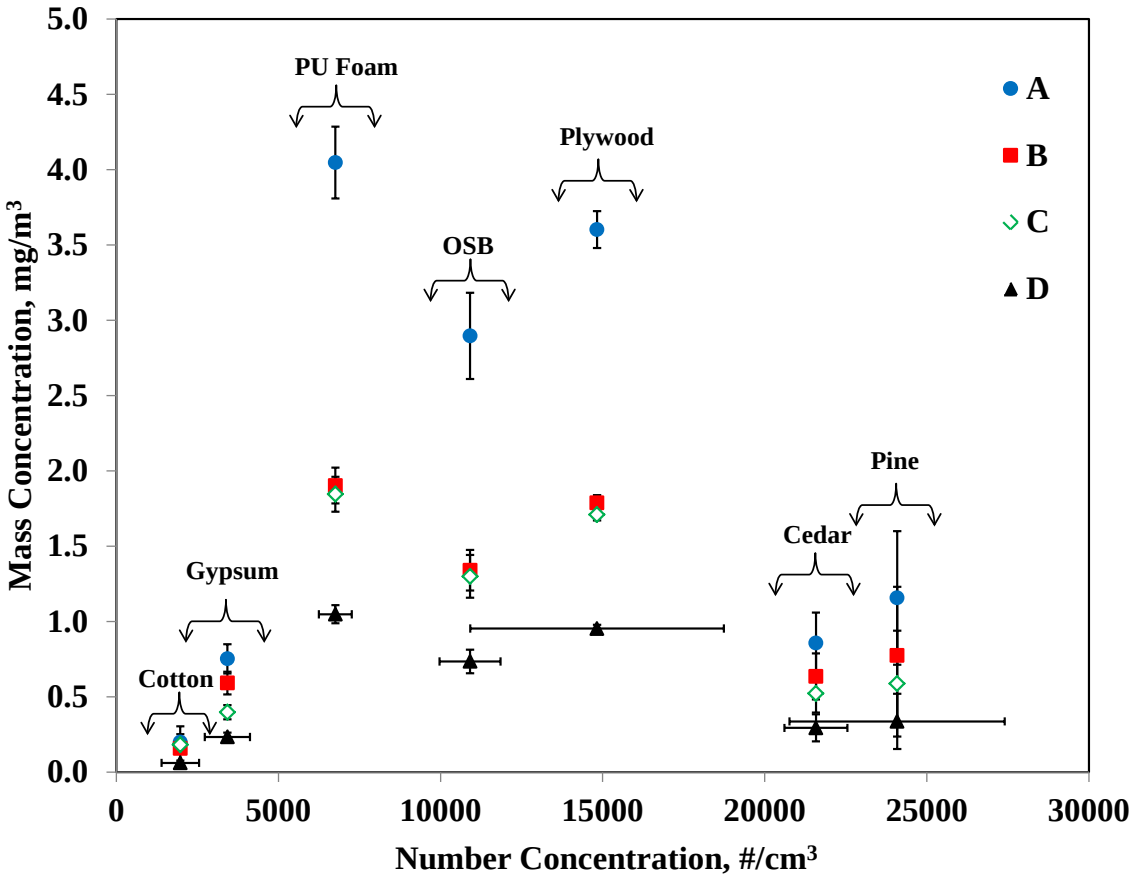

Figure 28 Sample averages of time averaged particle mass concentration (diluted) and number concentration (diluted). Error bars represent one standard deviation of the sample of repeat measurements.

Moving from left to right in Figure 28, the measured particle mass concentration increases with increasing particle number concentration, except for the untreated woods, cedar and pine. For

these two materials the average measured mass concentrations were low when compared to the large values of average number concentrations generated. Figure 15 and Figure 21 show that for cedar and pine, respectively, there were long periods of very low to negligible measured mass concentration during periods of very high number concentration. These were also periods of lowest CMD. Not only were there long periods of particles going undetected by the dust monitors, these long periods are in included in the time averaged mass concentration, biasing it toward zero.

The sample average of the CMD and GSD are listed in Table 2 for each of the materials, along with the sample average of measured mass concentration and number concentration. Comparing CMD and mass, the greater values of mass concentration correlate with larger measured CMD, consistent with larger particles having larger mass. For example PU Foam had the largest mass concentration and the largest CMD on average. The CMD for the untreated wood materials were at the low end of the range for the materials tested, but the untreated wood materials generated the greatest number of particles on average. Since small particles carry less mass, this is more evidence that the conventional means of detecting and evaluating a respiratory hazard may not be sufficient for environments that generate a mix of large and small particulates. Aerosol mass concentration is the current metric for exposure limits. Small particles are inhaled with more efficiency than large particles. Assuming that the particles generated during a fire are still present during overhaul, these results suggest that new metrics and tools for particle detection are necessary to limit exposures to small and potentially respirable particles.

Table 2 Sample mean ± standard deviation for repeat measurements of the time averaged particle CMD, GSD, mass concentration, and number concentration.

Materials	CMD (nm)	GSD (-)	Mass Conc. (mg/m^3)				No. Conc. (#/m^3)
			A	B	C	D	
Cotton Upholstery	131±2	1.30±0.01	0.20±0.05	0.16±0.04	0.18±0.12	0.06±0.02	1973±580
Cedar	134±2	1.30±0.01	0.89±0.20	0.64±0.15	0.52±0.13	0.29±0.09	21580±973
White Pine	135±10	1.30±0.02	1.16±0.44	0.78±0.46	0.59±0.35	0.34±0.18	24085±3319
Gypsum Board	135±12	1.30±0.06	0.75±0.10	0.59±0.08	0.40±0.05	0.23±0.03	3426±696
Plywood	157±3	1.30±0.01	3.60±0.12	1.79±0.05	1.71±0.04	0.95±0.03	14827±3911
OSB	157±3	1.30±0.01	2.90±0.29	1.34±0.14	1.30±0.14	0.74±0.08	10911±942
PU Foam	171±5	1.40±0.02	4.05±0.24	1.90±0.12	1.85±0.12	1.05±0.06	6757±508

CONCLUSIONS

The surrogate smokes investigated, induced linear responses from the dust monitors over the range of particle mass concentrations for which exposure threshold limits have been defined. However, for some of the detectors, the sensitivity varied with respect to the aerosol. Because there is a wide variety of aerosols in fire overhaul, finding a representative single surrogate aerosol may prove difficult. A mix of aerosols may be appropriate.

In order to try to simulate the types of particle present in the overhaul environment, seven materials were burned and the particulates generated during the burning were sampled. The response of each handheld dust monitor was unique for each material, however, the response across the devices were similar enough to categorize them with respect to types of materials. Three such categories defined here were fabrics and paper, polymers and engineered materials, and untreated wood products.

Rankings of the sensitivity of the dust monitors were consistent across materials. Instrument A had the greatest sensitivity, followed by instruments B, C, and D, in decreasing order. The responses of instruments B and C were generally equal. This was consistent with the results for the aerosolized mineral oil. These similar observations, suggest that aerosolized mineral oil is a potential surrogate smoke that may be useful to understanding how to rescale the factory calibrations of dust monitors for the overhaul environment.

For the untreated wood products, cedar and pine, the periods of the highest particle number concentration correlated to the periods of the lowest particle mass concentration and particle size. The untreated wood products generated the largest average number concentration, but low average mass concentration. Particle mass concentration is the current metric for threshold respiratory exposure limits. Since small particles are inhaled with more efficiency than large particles, the burning of untreated wood may create more of a respiratory hazard than the current metric would suggest. Assuming that all of the particles generated during the burning of untreated wood products are still present during overhaul, the results suggest that new metrics and tools for particle detection are necessary to limit respiratory exposures.

The cone calorimeter, a standard test apparatus used to determine the heat and smoke contribution to a fire from test materials, was used to generate smoke particulates from real materials. By following the standard test method, the apparatus provided consistent results for a specific material. Because the apparatus easily allows for particulate sampling of its exhaust and has an associated standard test method in place, it is a good candidate to use to further study the response of particulate detectors to burning materials.

RECOMMENDATIONS

The following list of recommendations is based on the knowledge gained from this work. It should provide a foundation for developing future research, standard testing protocols, and performance criteria that will allow the real-time particulate detector industry to improve and adapt the technology to the specific needs of firefighters and other first responders.

Future Work

1. Aerosolized mineral oil was demonstrated as a potential surrogate smoke. A study should be conducted to investigate using aerosolized mineral oil to calibrate dust monitors for use in the fire overhaul environment.
2. A real-time measurement of particle mass or mass concentration that is traceable to a standard gravimetric method of analysis, but is not an optical scattering method should be included in future studies. A real-time measurement that is not an optical scattering measurement provides an independent confirmation of mass concentration.
3. Since OPCs nominally measure particle size, uncertainty in the particle density gives rise to a proportional uncertainty in determining the measured mass exposure. Individual instruments may include provisions for inputting the particle density, while in other cases a default value is assumed. This aspect must be further investigated and quantified for aerosols or combinations of aerosols for which the density is not well known.
4. The measurement of particle size by optical scattering can be affected by the particle refractive index. In similarity to the previous consideration, some instruments are calibrated for a number of particle materials, whereas in other cases a default value is assumed. For this reason, a range of aerosols with differing values of refractive index must be examined. These tests must also address combinations of materials where the individual refractive indices may not be well known, or where the relative amounts of the individual materials may be unknown. The list of materials should be expanded beyond the list considered here, but it should be consistent with flammable materials found in buildings.
5. A chamber to increase the mixing of the smoke generated at different times in the burn (or from different burning events) should be added to future investigations. Such a chamber would allow the smoke to mix and age much like the smoke in the fire overhaul environment.
6. Since large amounts of water are used to extinguish a building fire, humidity levels can be high in the overhaul environment. Therefore, humidity and/or aerosolized water droplets should be added to the aerosol sample stream to investigate the effects on the detector response.

Metrics and Testing Protocols

1. Evaluate dust monitors to confirm a linear response of over the range of the current respiratory threshold limits, 0 mg/m^3 to 10 mg/m^3.
2. Coincidence errors arise when the number density of the aerosol becomes sufficiently large. For some OPCs, this can occur at number concentrations that are less than the corresponding allowable mass exposures. It is important that the concentration of test aerosols with a range of PSDs be varied to determine when this performance limit is reached for individual instruments.
3. Simultaneous measurements of particle concentration should be performed with a CPC in order to have a reference measurement of particle occurrence that is independent of particle characteristics such as size, shape, and refractive index.
4. The range of particle sizes that a specific OPC can measure can significantly affect the accuracy in determining mass exposure. Test aerosols and combinations of aerosols must address this consideration by virtue of having an appropriately wide range of PSDs.

5. Scale the dust monitor responses with a single surrogate smoke such as aerosolized mineral oil or other appropriate droplet.
6. Recommend using the cone calorimeter and standard test method ASTM E 1354-11a to generate real smoke particles. Smoke samples should be mixed and aged to better reflect the operation of sampling smoke with a handheld device in the overhaul environment.
7. Calibrations performed against real smoke particulates should use a real-time measurement of particle mass or mass concentration that is traceable to a standard gravimetric method of analysis.

Improvements for Real-Time Detector Technology

1) A dual device that can measure mass concentration and number concentration simultaneously would be ideal. When small particles dominate, mass concentration is low. Measurements of number concentration can still reflect the presence of a hazard. A good starting point is a particle counter that can convert its measurements to mass concentration with stated levels of accuracy.
2) The option to add an internal or external dilution system to optical particle counters could allow more of these devices to operate in high particle concentration environments like fire overhaul.
3) Including a standard list of calibration factors for different materials in the operation manuals of direct-reading particulate detectors would immediately show the user that care must be taken in interpreting the results while also offering a tool for better interpretation of the results. Aerosolized mineral oil could be one of the materials on the list.

REFERENCES

[1] T. LaTourrette, D. J. Peterson, J. T. Bartis, B. A. Jackson, and A. Houser, Protecting Emergency Responders: Community Views of Safety and Health Risks and Personal Protection Needs, **MR-1646** (2), RAND Corporation, Arlington, VA, (2003).

[2] J. L. Burgess, C. J. Nanson, D. M. Bolstad-Johnson, R. Gerkin, T. A. Hysong, R. C. Lantz, D. L. Sherrill, C. D. Crutchfield, S. F. Quan, A. M. Bernard, and M. L. Witten, Adverse Respiratory Effects Following Overhaul in Firefighters, Journal of Occupational and Environmental Medicine **43** (5), 467-473 (2001).

[3] D. M. Bolstad-Johnson, J. L. Burgess, C. D. Crutchfield, S. Storment, R. Gerkin, and J. R. Wilson, Characterization of Firefighter Exposures During Fire Overhaul, AIHAJ **61** (5), 636-641 (2000).

[4] P. Goerner, X. Simon, D. Bemer, and G. Liden, Workplace Aerosol Mass Concentration Measurement Using Optical Particle Counters, Journal of Environmental Monitoring **14** (2), 420-428 (2012).

[5] Workplace Exposure - Guide for the Use of Direct-Reading Instruments for Aerosol Monitoring - Part 2: Evaluation of Airborne Particle Concentrations Using Optical Particle Counters, **CEN/TR 16013-2:2010** European Committee for Standardization, Brussels, Belgium, (2010).

[6] R. A. Bryant, K. M. Butler, R. L. Vettori, and P. S. Greenberg, Real-Time Particulate Monitoring - Detecting Respiratory Threats for First Responders: Workshop Proceedings, **NIST Special Publication 1051** National Institute of Standards and Technology, Gaithersburg, MD, (2007).

[7] American Conference of Governmental Industrial Hygienists (ACGIH), Particle Size-Selective Sampling in the Workplace, **0830** ACGIH, Cincinnati, OH, (1985).

[8] American Conference of Governmental Industrial Hygienists (ACGIH), 2006 TLVs and BEIs, ACGIH, Cincinnati, OH, (2006).

[9] W. C. Hinds, Aerosol Technology: Properties, Behavior, and Measurement of Airborne Particles, **2nd** Wiley-Interscience, New York, (1999).

[10] Y.-S. Cheng and B. T. Chen, Aerosol Sampler Calibration, Air Sampling Instruments for Evaluation of Atmospheric Contaminants, **9th** (9), ACGIH, Cincinnati, OH, B. Cohen and C. McCammon, eds., 177-199 (2001).

[11] ASTM International, Standard Test Method for Heat and Visible Smoke Release Rates for Materials and Products Using an Oxygen Consumption Calorimeter, **E1354-11a** ASTM International, West Conshohocken, PA, 1-20 (2011).